JTTEE5 16:64–83
DOI: 10.1007/s11666-006-9007-2
1059-9630/$19.00 © ASM International

Peer Reviewed

Thermal Spray Coatings for Fusion Applications—Review

Jiří Matějíček, Pavel Chráska, and Jochen Linke

(Submitted December 22, 2005; in revised form June 26, 2006)

Thermonuclear fusion is a potential source of cleaner and safer energy for the future. Its technological realization depends on the development of materials able to survive and function in extreme conditions. This article reviews the applications of thermally sprayed coatings for fusion reactor materials. First, the principle and purpose of fusion is briefly introduced, and technological objectives are mentioned. Material-environment interactions are summarized, together with materials requirements and the role of coatings. Then, specific applications—e.g., the plasma facing components—are reviewed, focusing on application issues as well as issues related to thermal spray processing and specific properties of the respective materials. An overview of specific materials testing methods is also provided.

Keywords beryllium, boron carbide, plasma facing components, plasma sprayed coatings, thermonuclear fusion, tungsten

1. Introduction

1.1 Nuclear Fusion: Why and How

Nuclear fusion is a promising source of environmental friendly energy for the future, and one of the very few options available to solve the looming energy crisis. It offers significant advantages over other large scale sources—in particular its inherent safety, cheap and abundant fuel and minimum radioactive waste (Ref 1). Nuclear fusion is the subject of extensive internationally coordinated research, whose ultimate objective is to provide power generation means that is environmentally acceptable, economically viable, and can produce energy in sufficient quantities. The largest project today is the International Thermonuclear Experimental Reactor (ITER) (Ref 2, 3), for which the European Union (EU) and other states have already delimited financial resources, and its construction site has been selected. Its mission is to demonstrate the feasibility of thermonuclear fusion as a power source through an extended plasma burn in a tokamak and to verify the function of all necessary technologies in an integrated system for the next energy producing device.

The principle of nuclear fusion is the reaction of two light nuclei to form a heavier nucleus. Among those reactions that release energy, the most prospective is the fusion of deuterium and tritium (D-T), which produces helium and a neutron: $D + T \rightarrow He + n$.

J. Matějíček and **P. Chráska,** Institute of Plasma Physics, Praha, Czech Republic. Contact e-mail: jmatejic@ipp.cas.cz **J. Linke** Forschungszentrum Juelich, Juelich, Germany

The helium atom carries with it 4 MeV of energy, which is used for fuel heating, while the neutron carries 14 MeV, used for energy and tritium production. While other types of nuclear fusion reactions also have a potential for energy gain, the D-T reaction is the least difficult to initiate on earth. In order to achieve energy gain, a sufficient number of these reactions (collisions) have to take place. This translates to three factors: the fuel has to be kept at a sufficiently high temperature and concentration for a sufficiently long time. For the D-T reaction, the product of these three factors has to be above 10^{21} keV s/m^3 (Lawson's criterion) (Ref 4, 5). The role of technology is to provide such needed conditions, especially plasma heating and plasma confinement. The two approaches currently considered are inertial and magnetic confinement. In the inertial confinement, the fuel is rapidly heated (e.g., by a fast laser pulse), while the inertia of the particles would prevent them from escaping before the reaction happens. In the magnetic confinement, a complex magnetic field has to be applied to keep the hot plasma inside a toroidal vessel (tokamak or stellarator) without touching its walls. The applications for magnetic confinement will chiefly be considered here.

1.2 Materials and Coatings

The technological realization of a fusion power source is critically dependent on the successful development of high-performance materials (Ref 6). These materials will have to function in extreme conditions, being subjected to complex thermal, mechanical, and chemical loads as well as strong irradiation (Fig. 1). Material property changes with temperature and irradiation, component damage during service, and the need for repairs all add to the complexity of materials issues. As traditional construction materials are often at their limits, new materials are continually being sought. These include composites, layered structures, and coatings.

Currently developed and/or proposed coating applications include the following (Ref 7, 8):

Nomenclature

Processing techniques

APS	atmospheric plasma spraying
CAPS	controlled atmosphere plasma spraying
CDC	chemical densification coating
CVD	chemical vapor deposition
CVR	chemical vapor reaction
DJ	detonation jet spraying
HDA	hot-dip aluminizing
HIP	hot isostatic pressing
HPPS	high pressure plasma spraying
HSP	hybrid stabilized plasma
HT	heat treatment
LPPS	low pressure plasma spraying
LS	laser sintering
PM	powder metallurgy
PS	plasma spraying
PVD	physical vapor deposition
VPS	vacuum plasma spraying
WSP	water stabilized plasma

Materials

CFC	carbon fiber composite
FGM	functionally graded material
OFHC	oxygen-free high conductivity copper
SS	stainless steel

Materials properties

CTE	coefficient of thermal expansion
DBTT	ductile-brittle transition temperature
TC	thermal conductivity
T-PRF	tritium permeation reduction factor

Fusion-oriented devices

ASDEX	Axially Symmetric Divertor Experiment
CASTOR	Czech Academy of Sciences Torus
DEMO	Demonstration Reactor
FTU	Frascati Tokamak Upgrade
ITER	International Thermonuclear Experimental Reactor, also 'the way' in Latin
JET	Joint European Torus
NET	Next European Torus
SSPX	Sustained Spheromak Physics Experiment
TEXTOR	Tokamak Experiment for Technology Oriented Research
TJ-II	Tore Junta II
W7-X	Wendelstein 7-X

Terms related to fusion technology

ELM	edge localized mode
HHF	high heat flux
PFC	plasma facing component
PFM	plasma facing material
VDE	vertical displacement event

Miscellaneous

FEM	finite element modeling
RT	room temperature
SEM	scanning electron microscopy
T_S	substrate temperature
XRD	X-ray diffraction

- Plasma facing components to protect construction materials from particle and heat flux from the plasma
- Tritium barriers within the blanket system to reduce tritium permeation into water coolants
- Electrically insulating coatings to mitigate magneto-hydrodynamic effects in self-cooled liquid metal systems
- Tritium containment to reduce tritium release to the environment
- Corrosion barriers to permit higher temperature operation
- Helium containment to reduce helium leakage into the plasma chamber

The following are some general requirements/considerations for all coating systems (Ref 8):

- Potential for coating large complex configurations
- Processing parameters compatible with materials and capabilities, e.g., temperatures and times
- Thermal expansion matching and possibility of bonding with substrate

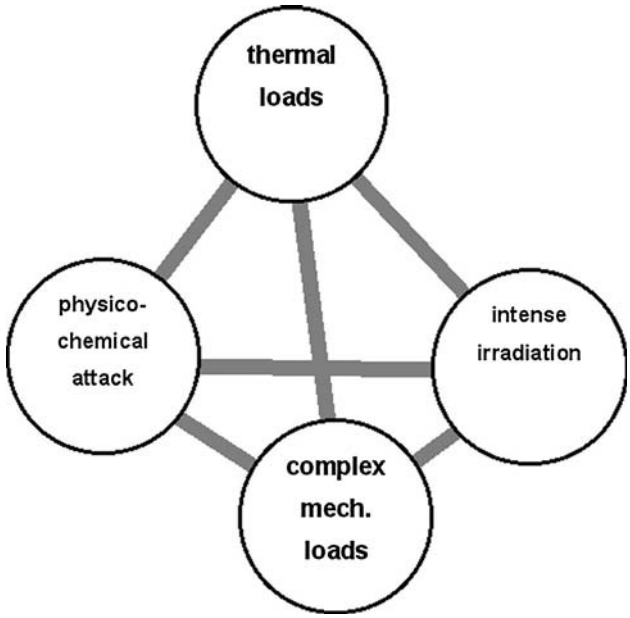

Fig. 1 Schematic of complex loading on fusion reactor materials. Image courtesy of Harald Bolt, Institute of Plasma Physics, Garching

- Acceptable neutronic properties
- Materials availability/cost
- Safety/environmental characteristics
- Radiation damage resistance
- Potential for in situ self-healing of defects that might occur

In most cases, the coating must be applied after the component assembly to avoid affecting the welding/joining and to assure effective coverage. For some applications, coatings are required, making them a feasibility issue, while for other applications they can enhance the performance, becoming an economic issue (Ref 9).

Thermal spraying as a coating deposition technology offers several advantages:

- A single-step manufacturing technology, thus eliminating the need for further joining
- Ability to coat large-area components, including complex shapes
- Prospect of in-situ repair of damaged parts
- Possibility to form graded composites
- Relatively low heat input to the coated parts
- Relatively low cost
- Relatively high coating thickness capability

Other coating techniques will also be mentioned below for specific application cases.

In the subsequent sections, the following applications and aspects will be reviewed: plasma facing components, hydrogen permeation barriers, electrical insulation, joining/stress relief and other special applications. The conditions in which the coatings have to function and the corresponding materials requirements and choices will be described. For specific materials, issues related to their thermal spray processing will be mentioned, as well as the relevant properties of the resulting coatings and their performance in fusion-oriented environments. For many of the materials presented here, thermal spraying research and development was conducted for other applications as well; but with a few exceptions of general importance, only those relevant for thermonuclear fusion are included.

2. Plasma Facing Components

2.1 Plasma-Material Interaction, Materials Requirements

Plasma facing components (PFCs) are subjected to particle and heat flux from the plasma and their role is to protect the underlying construction materials (Ref 8). The exact conditions in which they have to operate differ from device to device, so only a general overview is given here. The energetic ions and neutral particles escaping from the plasma impact on the plasma facing surface where erosion (by physical or chemical sputtering, evaporation or arcing), absorption, chemical bonding, and redeposition of the eroded material may take place (Ref 8, 10). The particles released back to the plasma would cause radiation losses that may terminate the discharge if too high. The heat flux from the plasma causes thermal stresses, which are superimposed on the residual stresses from the manufacturing, and a temperature increase of the surface which may lead to melting and/or evaporation or sublimation. For the past fusion devices, passive heat transfer through the PFCs was sufficient. However, in current and future devices, where high heat fluxes during long plasma discharges are to be removed, active cooling is necessary. Besides steady state operation, a number of off-normal events is foreseen, during which the PFCs will be subjected to increased heat loads and severe thermal shocks. These include disruptions (i.e., abrupt terminations of the plasma current), vertical displacement events (VDEs—uncontrolled shift of the plasma column) and ELMs (edge localized modes—controlled ''cleaning'' of the plasma from impurities) (Ref 11, 12). The development of materials able to withstand these events is carried out in parallel with the development of methods of better plasma control. Nevertheless, erosion of plasma facing materials (PFM) is to be expected (Ref 13). Therefore, sufficient material thickness has to be provided (around 3 mm for the divertor (Ref 14)) and a limited lifetime considered in the design. In fusion reactors with significant neutron flux, neutron irradiation will change the mechanical and thermal properties and can also induce dimensional changes (Ref 8).

The requirements for PFM could be briefly summarized as follows (Ref 10, 12, 15):

- Compatibility with the plasma and the underlying materials
- High temperature stability
- High erosion resistance
- High fracture toughness and thermal shock resistance
- High thermal conductivity
- Low irradiation changes
- Low tritium retention

2.2 Development of Plasma Facing Materials

The history of PFM, summarized in Ref 15, will be briefly recalled here. In the early stages of fusion research, the importance of plasma-material interaction was not yet fully understood, thus, the vessel material (typically stainless steel or nickel alloy) served also as the plasma facing surface. Precleaning of this surface from impurities like oxygen and carbon was applied prior to discharge, using various techniques. Limiters from refractory metals were used to protect the vessel from unstable discharges. However, impurities with a high atomic number (Z) caused high radiative power losses when they reached the plasma. In the 1970s, carbon was considered because of its low Z and high sublimation temperature. Extensive studies revealed a number of disadvantages, however. These included high rates of chemical sputtering by hydrogen, radiation enhanced sublimation, and occasional large influxes of carbon to the core plasma from localized hot

Table 1 Overview of ITER plasma facing materials and operating conditions

	Be	CFC	W	Ref
Components	First wall	Divertor vertical target	Divertor components	18
Permissible concentration in plasma	$\sim 10^{-2}$	$\sim 10^{-2}$	$\sim 10^{-6}$	19
Melting point (°C)	1285	3500 (subl.)	3410	20
Max. steady-state surface temperature (°C)	800	1500	1500	12
Foreseen operational temperature (°C)	200-300	200-1500	200-1000	8
Heat flux under normal conditions (MW/m^2)	0.5	5-10	0.1-5	8, 11, 21
Heat flux during transient events (MW/m^2)				8, 11
Disruptions	...	<30,000	<30,000	
VDEs	60-200	...	...	
ELMs	...	<500	<500	
Energy density (MJ/m^2)/pulse duration (ms) during transient events				21
Disruptions	1/0.1-3	10-30/0.1-3	10-30/0.1-3	
VDEs	60/100-300	60/100-300	60/100-300	
ELMs	?	1/0.1-0.5	1/0.1-0.5	
Estimated erosion (mm/year)	3-10	...	0.03-0.3	8

Note: A practical comparison of advantages and disadvantages of these three materials can be found in Ref 22. Be: Beryllium; CFC: Carbon fiber composite; W: Tungsten; Ref: References.

spots (Ref 15); also high erosion rates at elevated temperatures, degradation of thermal conductivity by neutron damage and high tritium retention (Ref 16). Several coating and surface conditioning techniques were then developed, including carbonization, boronization and siliconization, to reduce the influx of impurities from the walls. As these coatings could not be used for longer pulses due to easy erosion, beryllium became a prime candidate. Its advantages include low Z, oxygen gettering ability, absence of chemical sputtering, and low hydrogen inventory. Tungsten has been considered recently, mainly due to its higher erosion resistance compared to low Z materials (Ref 8, 17).

In today's numerous fusion-oriented devices, which vary in pulse length, plasma density, plasma temperature and other technological features, practically all the above mentioned materials are used, from a bare stainless steel wall to several materials combinations. The ITER design considers three materials for its PFCs: beryllium for the first wall, and tungsten and carbon fiber composite for the divertor (Table 1, Fig. 2). The first wall/blanket absorbs the heat radiating from the plasma and provides neutron shielding. The divertor exhausts the flow of energy from charged particles produced in the fusion reactions and removes helium and other impurities (Ref 3). Basic properties of the materials relevant for PFCs are summarized in Table 2.

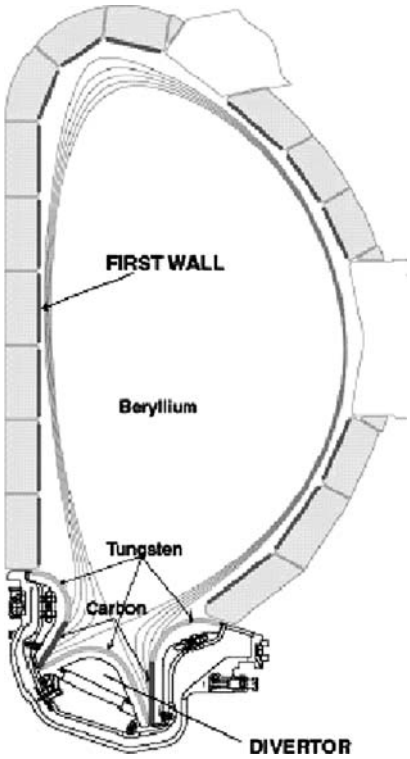

Fig. 2 Cross section of the plasma facing components inside the ITER vessel—first wall/blanket and divertor—where plasma spraying can be applied. Image courtesy of Mario Merola, ITER

2.3 Ceramics

Plasma sprayed Al_2O_3, TiO_2, and TiC coatings were considered as materials for the first wall of the Next European Torus (NET), due to their low Z and refractory nature (Ref 38). The goal was to achieve a low thermal conductivity, to act as a thermal barrier. Decarburization and oxidation were observed when spraying TiC by APS (Ref 39). When tested under high heat fluxes, induced by an electron beam gun (Table 3), TiC was found to be too brittle, while the other two materials performed better. Thermal shock resistance of TiC coatings can be enhanced by preheating the substrate, application of a bondcoat and macroroughening the substrate, where the grooves act as crack stoppers (Ref 40). Also, low nitrogen and oxygen content (in VPS coatings) was found to be beneficial (Ref 56). Thicker coatings with intermediate porosity were found to have lower relative crack propagation (Ref 39).

Table 2 Selected basic properties of important thermally sprayable fusion reactor materials

Property	B_4C	Ref	Be	Ref	W	Ref	Cu	Ref
Density	2.52	23	1.85	24	19.3	25	8.9	25
Melting point (°C)	2450	26	1280	24	3410	25	1080	25
Boiling point (°C)	>3500	27	2470	24	5930	28	2350	29
Thermal expansion (10^{-6} C^{-1})	4.5	23	11.5	30	4.5	25	16.6	25
Specific heat (J/kg C)	970	26	1925	30	140	25	390	25
Heat of fusion (kJ/kg)	1867	25	1130-1350	24, 30	184	30	205	29
Thermal conductivity (W/m C)	27-36	31	201	24	145-163	25, 30	400	25
Hardness (GPa)	26-38	23	1.5-2	32, 33	3-5	29, 30	0.8-1	29
Flexural/tensile strength (MPa)	350-480	23	480	30	1000	25	210	25
Young's modulus (GPa)	370-470	23	307	30	410	25	130	33
Shear modulus (GPa)	160-200	23	135	30	156	30	48	33
Poisson's ratio	0.17	23	0.07-0.18	30	0.28	25	0.33	25
Electrical resistivity (Ω cm)	0.1-10	30	4.3×10^{-6}	30	5.6×10^{-6}	30	1.7×10^{-6}	30
Sputtering yield under deuterium bombardment	0.04-0.07	34	$\sim 10^{-3}$	15	$\sim 10^{-4}$	15	···	···
Threshold energy for sputtering by hydrogen isotopes (eV)	···	···	9	15	220	15	···	···
Cross section for thermal neutrons (barn)	600	35	0.1-10	36	18.5	25	3.8	25

Note: A wider spectrum of relevant materials can be found in Ref 37.

Boron carbide is an important fusion reactor material that has been subjected to extensive studies. Its advantages include low *Z*, a relatively high melting point, thermal shock resistance, low vapor pressure, oxygen gettering, chemical inertness, and easy hydrogen isotope release (Ref 42, 51, 57). Compared to carbon, it has lower chemical and high temperature erosion sputtering, lower hydrogen recycling, and is also an oxygen getter (Ref 58, 59). Due to high absorption of neutrons (because of boron), however, it could not be used as plasma facing material in reactors with significant neutron flux. Another drawback is the relatively low thermal conductivity of plasma sprayed boron carbide layers. Plasma sprayed B_4C coatings have been already tested in Tore Supra tokamak (Ref 42) and are planned for the first wall coverage of the Wendelstein 7-X stellarator (Ref 54).

Boron carbide, with its high melting point, high specific heat, high melting enthalpy and low density is a very challenging material for plasma spraying (Ref 26). For such a lightweight material, powder injection is crucial. Better melting was observed with a higher content of H_2 in plasma gas (Ref 26, 60). Plasma spraying in air is accompanied by oxidation (B_4C starts to oxidize at 600-800 °C (Ref 61, 62)); consequently, the resulting coatings are often porous and brittle and contain B_2O_3 (Ref 41, 51). Shrouding by inert gases provides only moderate improvement (Ref 51). Better results are generally obtained by spraying in a controlled atmosphere (Ar) or vacuum (Ref 41, 43, 45). Still, very dense APS coatings were reported in Ref 48. For good heat transfer and thermal shock resistance, B_4C coating thickness has to be rather low (Ref 31), compliant bondcoat or graded interlayer is necessary for higher topcoat thickness (Ref 41, 43, 46, 47, 49, 63). Due to its relatively low CTE, the coatings are typically under compressive stress (Ref 54, 63, 64). Rather thick coatings were produced by spraying in inert gas at high pressures (up to 200 kPa) (Ref 44). High pressure spraying features a denser plasma jet, thus higher energy density and temperature, lower velocity and better heat transfer, compared to VPS or APS. Denser coatings were achieved at higher chamber pressures and higher substrate temperatures (Ref 45). Better adhesion was also achieved at high substrate temperatures (Ref 64). For the next step stellarator Wendelstein 7-X, B_4C coatings are to be applied on 3D wall components with complicated shapes. Therefore, spray angle becomes an important factor. In Ref 53, its effects on various coating properties during VPS were studied. Increasing spray angle resulted in an asymmetric splat formation, increasing porosity and roughness and accordingly decreasing hardness and modulus. However, the off-angle coatings exhibited better thermal shock resistance in disruption simulation tests, which may be related to higher thermal conductivity along the differently shaped lamellae.

Early plasma sprayed B_4C coatings (Ref 65) showed good performance under steady heat loads up to the melting point when sprayed on graphite (with similar CTE); cracking occurred in coatings sprayed on Mo where the CTE mismatch was higher. However, they showed limited capability to withstand disruption-like loads in the MJ/m^2 range, with substrate melting. In another disruption simulation test (Ref 66), coatings on CFC suffered higher erosion than uncoated CFC, but the substrates remained unaffected. Formation of hot spots and delamination at pre-existing defects was a typical failure mechanism (Ref 46). Further coating developments have led to increased heat flux resistance, despite the low thermal conductivity (see Table 3) (Ref 50, 52, 54). Disruption simulation tests have shown that some surface melting can be tolerated without gross coating failure (cracking, delamination, burn-through) (Ref 43, 67). Preferential evaporation of boron from the melted regions was observed in some cases (Ref 68). Coatings produced

Table 3 Summary of properties and performance of ceramic coatings as plasma facing materials

Material	Technique	Thickness, mm	Substrate	Density, %	TC, %	E, GPa	Damage threshold under heat flux, $MW/m^2\ s^{0.5}$/cycles	Ref
Al_2O_3	APS	0.12-0.2	Al, SS, Cu	···	···	···	0.4-0.8	38
TiO_2	APS	0.03-0.05	SS, Cu	···	···	···	<0.4	38
TiC	VPS	0.05-0.12	Al, SS, Cu	94	···	···	0.1-0.2	38
TiC	APS, VPS, LPPS	0.3-1.3	Steel, SS	74-92	···	···	0.3	39
TiC	PS	0.9-1	Inconel	85	13	···	5-9	40
B_4C	LPPS	0.2	Mo, graphite	85-92	···	···	···	31
B_4C	LPPS	0.13-0.25	Mo, graphite, CFC	85-92	···	···	9	38
B_4C	CAPS	0.4	SS	89-91	···	···	···	41
B_4C	PS	0.05-0.2	CuCrZr	···	4	···	38	42
B_4C	CAPS	0.3	Al	63-86	···	···	···	26
B_4C	CAPS	0.3-1.5	SS	···	4	···	22; 20/100	43
B_4C	HPPS	Up to 4	Steel, graphite	Up to 88	···	···	···	44
B_4C	HPPS	···	Ti, steel	85-92	···	75-130	···	45
B_4C	HPPS	1.2	SS	···	8	···	6	46
B_4C	VPS	0.5-1.5	SS	86	3	50	···	47
B_4C	APS	0.2	SS	96	···	230	···	48
B_4C	PS	0.3-0.4	Cu	···	···	···	6.4/1000	49
B_4C	CAPS	0.15	Cu	90	5	···	7.5/1000	50
B_4C	APS-WSP	0.1-1	Steel, SS	51-95	···	40-70	···	51
B_4C	VPS	0.5	···	···	>4	···	6.7/1000; 15	52
B_4C	VPS 90°	0.16-0.2	SS	89-93	···	170-210	···	53
B_4C	VPS 30°	0.16-0.2	SS	78-85	···	130-160	···	53
B_4C	VPS	0.3-0.5	SS	65-95	7	220-270	6.7/1000	54

Note: For comparison, density and thermal conductivity are presented as percentage of bulk material (cf. Table 2). SS = stainless steel, CFC = carbon fiber composite. To allow for a comparison of heat flux test results of varying power and duration, the unit $MW/m^2\ s^{0.5}$ is used, which is proportional to the surface temperature increase (Ref 40, 55). Where no number of cycles is presented, tests were performed with a single loading.

by chemical vapor reaction (CVR) showed better heat flux performance than LPPS or CVD coatings, making them suitable for the divertor of JT-60 tokamak (Ref 68). Extensive testing of VPS B_4C coatings with a mixed B_4C/SS interlayer (Ref 54) revealed that they are suitable for coverage of the first wall of Wendelstein W7-X, ensuring reliable adhesion, heat flux erosion resistance and good dielectric properties. VPS B_4C coatings (with and without Cu or NiCr interlayer), developed for heat shields of TJ-II stellarator's neutral beam injection system showed good results with respect to the uniformity, roughness, and adhesion of the boron carbide layer and no significant changes in the thermal and mechanical properties under neutral beam and hydrogen beam irradiation (Ref 69).

When LPPS B_4C coated graphite tiles were exposed to plasma in JET tokamak, localized melting was observed in regions where the temperatures recurrently reached ~2000 °C; chemical analyses suggested preferential sublimation of boron (Ref 70). Plasma sprayed B_4C limiters for W7-X were also exposed to plasma in tokamak Textor (Ref 59, 71). Their heat flux resistance was comparable to coat mix bulk material (B_4C grains in a carbonized epoxy matrix), but inferior to conversion coatings (produced by a heat treatment of boron and carbon containing precursor) (Ref 71). Despite early melting, the entire area remained covered with B_4C. Localized erosion (melting of the top layer as well as the underlying copper) due to arcing was observed in other tests (Ref 59). As B_4C has electrical resistivity that decreases with increasing temperature, repeated arc attachment was related to irreversible changes in conductivity in the arc attachment regions.

Besides plasma spraying and those mentioned above, a number of other techniques has been used for production of B_4C surface layers, such as hot pressing (Ref 72), cold isostatic pressing (Ref 73), reaction sintering (Ref 74), CVD (Ref 75), and gas conversion (Ref 58). An overview of coatings produced by various techniques, including their erosion, hydrogen transport and heat flux properties, is provided in Ref 58. In this reference, CVD coatings were proposed as the most promising candidates for B_4C application in tokamaks, mainly due to their heat load resistance. On the other hand, thick CVD coatings would behave brittle like a bulk material, while plasma sprayed B_4C might have the advantage of higher strain tolerance.

2.4 Beryllium

Beryllium is considered as a neutron multiplier material in solid breeder blankets, as a (solid) plasma-facing material for ITER; also, in the form of the molten salt mixture of LiF and BeF_2 (commonly called FLIBE) as a renewable plasma-facing surface in advanced concepts for fusion reactors and also as a coolant (Ref 76). Beryllium has advantages including a lower Z number than carbon, in situ reparability by plasma spraying, oxygen gettering ability, etc. (Ref 15, 76). Disadvantages include its low melting temperature and high vapor pressure, its high physical sputtering yield, mechanical property degradation during neutron irradiation, chemical reactivity with steam

Table 4 Summary of properties and performance of beryllium coatings as plasma facing materials

Technique	Thickness, mm	Substrate	Density, %	TC, %	MW/m^2 s$^{0.5}$/cycles	Ref
LPPS	10	Cu	95	35-72	···	77
VPS, T_s = 500 C	12	Be	90	67	···	78
VPS, T_s = 800 C	12	Be	98	94	···	78
VPS	15	Cu alloys	···	···	4.5/3000	79
LPPS	5, 10	CuCrZr	99.5	···	···	80

TC: Thermal conductivity; Ref: References.

and relatively slow tritium release kinetics (Ref 76). Due to its toxicity and difficult handling, the number of laboratories able to spray beryllium is very limited.

Beryllium is currently considered as a material for the first wall of ITER, which will have a plasma facing surface of about 700 m^2 (Ref 3). Coating such an area with 5-10 mm of Be by plasma spraying would require about 10 t of powder (Ref 77). Plasma spraying can replace costly machining and alignment of modules (Ref 78). LPPS has been the preferred technology, because of its ability to spray reactive materials in a protective atmosphere, higher particle velocities, and the possibility of a transferred arc cleaning/heating of the substrate, improving the coating density and adhesion (Ref 77). Optimization of the spraying process was done with the help of numerical modeling of the plasma-particle interaction at various operating pressures. The results predict higher particle temperatures and velocities at lower pressures (Ref 24). The coatings should have high thermal conductivity, to maximize the heat transfer through the coatings (Ref 78). Better purity powder was found to form higher thermal conductivity coatings (Table 4); impurities can also form brittle intermetallics at the interfaces and cause cracking (Ref 77). About 30% higher thermal conductivity was observed in the in-plane than in the transverse direction. Increased substrate temperatures improved the thermal conductivity and bond strength of the coatings (Ref 78). Oxide layers were observed at splat interfaces, even with VPS. At higher temperatures, the coatings featured larger grains, fewer interfaces and interfacial oxides, all leading to improved thermal conductivity. Also, metallurgical bonding and epitaxial growth were observed, compared to predominant mechanical interlocking at low substrate temperatures (Ref 78). Plasma-sprayed beryllium ITER first wall mock-ups have survived 3000 thermal fatigue cycles at 1 MW/m^2 without damage, which is twice the expected peak heat flux for the ITER primary first wall modules (0.5 MW/m^2) (Ref 79). The failure occurred by lateral cracks in the coating, in porous layers associated with individual torch passes, thereby reducing the through-thickness thermal conductivity.

LPPS was also used to deposit 5 and 10 mm beryllium coatings on copper substrate mock-ups for high heat flux testing (Ref 80). Coatings of this thickness require special substrate surface preparation to ensure adhesion, as thermal mismatch stresses build up, imposing large shear stresses at the interface. From several anchoring options, a pattern of rising cubes with a height of 30% coating thickness were chosen for best performance. For an estimate whether Be coating of such thickness would survive deposition in one step, stainless steel (with similar CTE) was sprayed first as a surrogate material. Well-adherent Be coatings were deposited, showing only a small amount of globular porosity and requiring minimal post-spray machining.

The porous nature of plasma sprayed beryllium is responsible for a higher impurity content and higher temperature required for outgassing, compared to hot-pressed PM material (Ref 81). On the other hand, less deuterium is retained in plasma-sprayed samples, presumably due to the columnar structure of the resultant sprayed material that contains enhanced pathways to the sample surface.

2.5 Tungsten

Tungsten is one of the two candidate materials (with CFC) for the ITER divertor (Ref 17) and the main candidate material for the next step device (DEMO) (Ref 8). It is currently the most frequently studied from plasma sprayed materials for fusion applications (Table 5). Tungsten has the highest melting point of all metals, the lowest vapor pressure, good thermal conductivity and high temperature strength and dimensional stability; also, it does not form hydrides or co-deposits with tritium (Ref 17, 25). It has much higher atomic number than carbon or beryllium, making it a highly undesirable impurity in the plasma (Table 1). On the other hand, it has also much higher threshold energy for sputtering as well as sputtering yield, largely due to its high atomic weight (Ref 15). Among its disadvantages are the ductile-to-brittle transition (Ref 25), embrittlement under neutron irradiation (Ref 17), difficult machining and welding (Ref 16). For improved mechanical properties, alloys and pseudo-alloys are considered. A comprehensive summary of relevant properties of tungsten and its alloys is provided in Ref 25.

In plasma spraying, although the energy required to melt a unit mass of tungsten is comparable to other common metals, its high density leads to higher required energy per unit volume. Thus, finer powder particles are typically used (Ref 83). Also for its high density, carrier gas quantity must be adjusted carefully (Ref 85). Similar to boron carbide, plasma spraying in air is complicated by in-flight oxidation. Coatings sprayed in Ar had significantly higher interlamellar bonding and thermal conductivity than those sprayed in air (Ref 84). A detailed study of the oxidation phenomena was undertaken, using numerical modeling complemented by experimental observation (Ref 97). The model considered the heat and

Table 5 Summary of properties and performance of tungsten coatings as plasma facing materials

Technique	Thickness, mm	Substrate	Density, %	TC, %	Modulus, GPa	Damage threshold under heat flux, $MW/m^2\ s^{0.5}$/cycles	Ref
VPS	0.2-0.45	Cu, SS	90	...	...	10	38
VPS	0.1-0.35	Cu, SS	90	...	...	0.3-1.4	82
LPPS	2.5-4	Cu, SS, graphite	90	60	280-300	...	83
APS	...	Cu	84	5	...	...	84
CAPS	...	Cu	86	12	...	...	84
LPPS	~0.5	Cu	88-92	...	...	...	85
CAPS	0.1-0.2	Graphite	...	...	...	22-23	55
VPS	0.13-0.5	Graphite	...	...	...	12-15	55
VPS + HT	0.25-0.5	Graphite	...	...	...	15-22	55
CAPS	0.2	Graphite	80-85	...	...	...	55
VPS	0.5	Graphite	91-92	...	...	...	86
CAPS	4	CuCrZr	92	27-53	65	16/1000; 22	87
VPS	2	Mo	92	...	...	...	88
VPS	0.5-1	CFC, graphite	92.5	...	...	...	16
LPPS	1	Mo alloy	>90	...	...	66/4	89
VPS	0.1	Mo alloy	98	...	...	...	90
VPS	3-5	CuCrZr	...	27	...	4/1000	50
	5	CuCrZr	90	70	...	...	91
VPS	0.5	CFC	92.5	...	...	57/1000; 95/230	92
CAPS	0.5	Graphite	84	...	...	57/1000	92
VPS	2	Steel, Mo	80, 97	13, ~100	120	43/10	93
APS	0.6	Graphite	94-96	4	...	...	94
APS-WSP	0.3-0.5	Steel, Cu	80-85	<80	60-150	35-50	95
APS-HSP	0.5	Steel	94-96	20-60	80-90	...	96

TC: Thermal conductivity; Ref: References.

mass transfer in a simplified representation of the spraying process, for two cases—pure tungsten and tungsten covered with WO_3. Tungsten oxidizes readily above 400 °C (Ref 98); the melting and evaporation temperatures of WO_3 are 1470 °C and 1840 °C, respectively (Ref 33). This is well below the melting point of tungsten (3410 °C). The results indicate the following scenario: As tungsten particles travel in a mixture of plasma gas and air, oxide forms on their surface and quickly melts and evaporates. The evaporation consumes a significant portion of the heat, transferred to the particle from the plasma, and the vapor cloud reduces the heat transfer as well, resulting in incomplete melting of some particles. Only moderate improvements were achieved with inert gas shrouding or an admixture of tungsten carbide (Ref 97), Fig. 3, in which the carbon creates an auto-shrouding effect (Ref 99). On the other hand, the low evaporation temperature of WO_3 is responsible for the relatively small oxide content in the coatings, typically around 0.1% (Ref 84, 97). When substrate cooling and/or shrouding is applied, this is found only on the coating surface, while inside, the oxide content is several times lower (Ref 96). Both lower porosity and lower oxide content (compared to water stabilized torch coatings) were achieved using hybrid torch with argon and water stabilization, whose plasma jet is more stable, longer and with lower temperature gradients (Ref 96). Using higher torch power resulted in higher oxide content, but lower porosity coatings (Ref 94). In view of the above, it is not surprising that tungsten is sprayed mostly in inert gas (Ref 55, 64) or vacuum (Ref 16, 92). Vacuum also allows for using high deposition temperatures, resulting in low porosity and high thermal conductivity coatings (Ref 93). Still, even in VPS coatings, oxygen and carbon impurities can be found (Ref 93).

As tungsten is to be applied for plasma facing components, its thermal conductivity is of crucial importance, since it controls the temperature gradient and therefore the surface temperature of the components during operation (Ref 83). In a detailed study (Ref 84), it was related to the coating microstructure, with the help of analytical calculations and copper infiltration to visualize the interfaces and voids. While coatings sprayed at different conditions had only small differences in porosity, markedly different thermal conductivities were measured. It was strongly correlated to the bonding ratio between the lamellae; the presence of a thin oxide layer at the interfaces was concluded to have little influence. Thicker lamellae led to higher thermal conductivity, as there were fewer thermally resistant interfaces through the coating thickness (Ref 84). From a technological point of view, the spraying atmosphere, torch traverse velocity and powder feed rate were found to have a strong influence (Ref 100).

As a candidate plasma facing material, W-SiC composite was also produced by APS (Ref 101), the carbide being advantageous for its high thermal conductivity and high chemical stability. Partial melting and decomposition of SiC were responsible for increased porosity, but no formation of tungsten silicide or carbides was observed.

Since tungsten has largely different mechanical and thermal properties than most typical substrate materials, large stresses at the interface may occur (Ref 102). To reduce the stress concentration, graded or composite interlayers are being applied. This concerns mainly tungsten

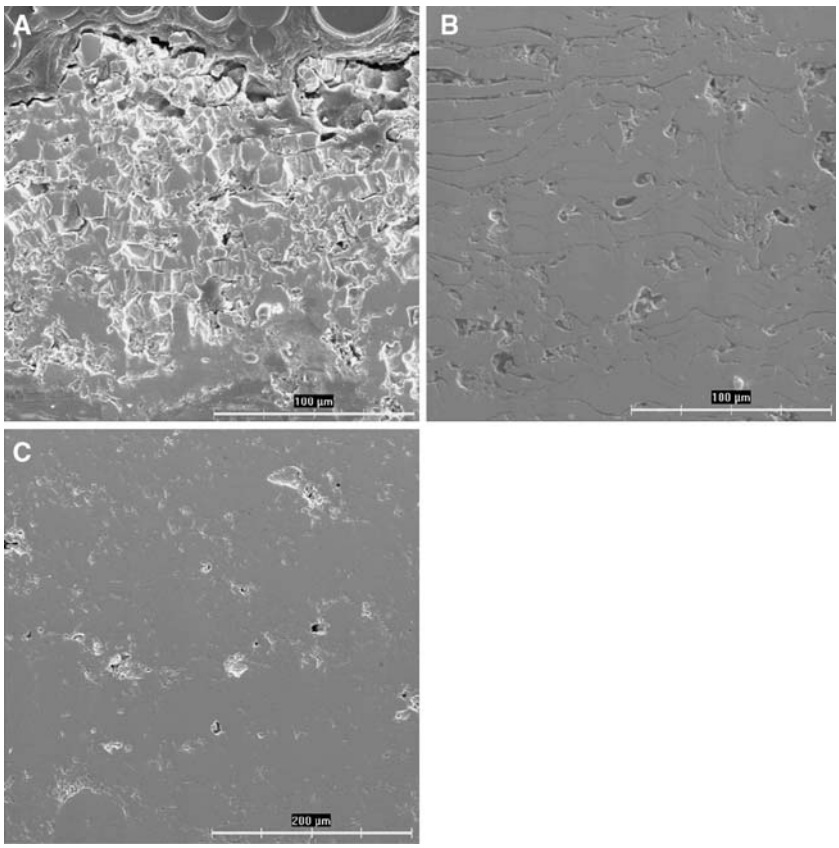

Fig. 3 Examples of structures of atmospheric plasma sprayed tungsten coatings, illustrating the effect of different spraying parameters: (a) pure W, WSP, 60-350, (b) W + WC 5:1, WSP, 40-250, (c) pure W, HSP, 25-250. The first number refers to the feeding distance, the second to the spraying distance (mm)

and copper, to which a special section (Section 5.1) will be devoted. Residual stresses in the coating are affected by the deposition temperature, CTEs and moduli of the tungsten coating as well as the interlayer (Ref 103). To avoid brittle carbide formation at the interface with carbon-based materials (graphite, CFC), a thin diffusion barrier layer (Re, Si) is sometimes applied (Ref 16, 55).

VPS, CAPS, and PVD tungsten coatings on graphite were investigated in Ref 55 and tested under high heat loads. The thermal response, damage thresholds and failure mechanisms were connected to specific structure of the coatings. Relatively high porosity of the CAPS coatings reduces their thermal conductivity, but on the other hand also reduces the thermomechanical stress and provides crack-arresting sites. The denser VPS coatings exhibit higher conductivity and also higher strength; this leads to high elastic energy stored in the coating during the heat load and thus fast crack propagation. Unmolten particles in the coating may act as crack initiators and also reduce the adhesion. Typical columnar structure of dense PVD coatings possibly may have also promoted the cracking. All the PS coatings were able to withstand cyclic loading of 10 MW/m^2 for 1000 cycles. Crossing DBTT had no influence on the lifetime of PS coatings. Similar behavior was also observed in Ref 92, where VPS, CAPS, and powder metallurgy (PM) W materials on CFC and graphite were studied. Local cracks occurred in CAPS (parallel to the surface), but did not propagate, probably due to the crack-arresting effect of the pores. The cracks propagated only in VPS and bulk samples at extremely high heat fluxes (>55 MW/m^2). The VPS W suffered higher weight loss than bulk W but lower than CFC. Dominant erosion mechanisms were particle emission for the PS and evaporation for bulk material (Ref 104). Although W-Re interlayer was applied by PVD, the boundaries disappeared on annealing and WC phase formed at the interface at temperatures over 1600 °C (Ref 92). Heat flux tests of WSP-sprayed W coatings indicated a damage threshold of ~0.5 GW/m^2 in thermal shock loads (pulse duration 5-10 ms) (Ref 95), Fig. 4. The main damage mechanism was melting and localized delamination, attributed to the low thermal conductivity. The least damage was observed in the highest thermal conductivity specimen. However, no cracking was observed, contrary to bulk tungsten (Ref 105). In another study involving heat flux testing of VPS coatings on CFC and graphite (Ref 16), a negligible difference in surface temperature vs. heat flux was observed between coated and uncoated samples, indicating good adhesion and thermal conductivity. Vertical cracks were found after exposure, without loss of overall integrity and degradation of thermal conduction. No delamination was observed up to the melting point (Ref 106).

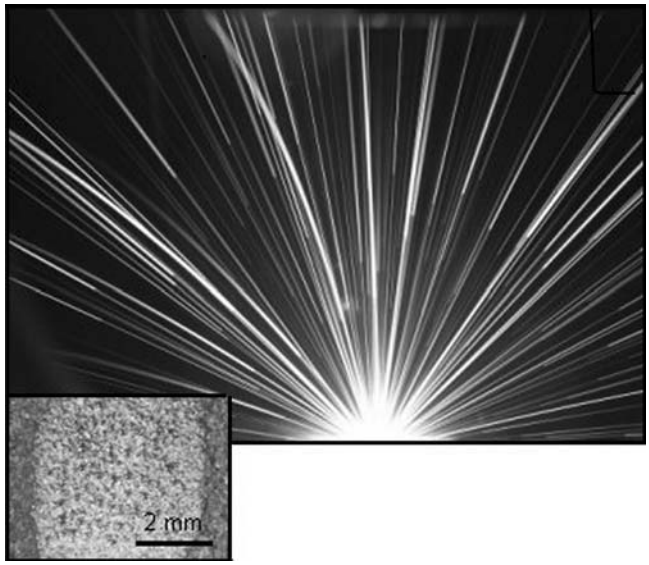

Fig. 4 Example of particle emission during an electron beam thermal shock loading on plasma sprayed tungsten. Curved trajectories correspond to heavier tungsten droplets. Insert: irradiated surface (Ref 95)

Small size, actively cooled mock-ups for the ITER divertor, manufactured by VPS and other techniques, were heat flux tested in Ref 91. Their damage threshold (5 MW/m^2, 1000 cycles) was lower than for those based on bulk tungsten; the failure occurred due to impurities at the interface. Real size mock-ups of a baffle module for ITER were produced by VPS; as-sprayed and castellated (with vertical slits machined in the surface) specimens were tested under heat flux with active cooling. Both types sustained nearly 2000 cycles at 4 MW/m^2 (Ref 107).

When the performance of the coatings developed in Ref 55 was tested during the actual operation in ASDEX-U Ref 108, the results confirmed the damage mechanisms determined in heat load tests (Ref 55). The VPS coating turned out to be the best option, having had a higher damage threshold; the more porous CAPS coating did not crack, but started to melt due to lower thermal conductivity (Ref 108). Despite extensive cracking, there was no influence on plasma performance or on tungsten concentration in the plasma (Ref 109). The tungsten erosion was dominated by light intrinsic impurities and typical tungsten concentrations in the main plasma were sufficiently low for a burning plasma (Ref 110). The study in Ref 111 suggests that it undergoes a prompt local redeposition and that its throughput by erosion and subsequent non-local redeposition is at least a factor of 100 smaller than for carbon or beryllium.

A tungsten coated molybdenum poloidal limiter has been tested in the FTU tokamak (Ref 88). It received energy densities as high as 3 MJ/m^2 during steady state discharges and up to 6.5 MJ/m^2 during disruptions, resulting in melting and ablation in certain zones, but no macroscopic damage in most of the area. In Ref 112, high-pressure plasma sprayed tungsten was applied on copper substrates as PFCs of the Sustained Spheromak Physics Experiment (SSPX). The porous coating structure was capable of retaining high levels of water, but cleaning techniques such as baking, glow discharge, and shot conditioning reduced the impurity content considerably. WSP sprayed W coatings tested in the tokamak CASTOR showed negligible influence on the plasma discharge up to relatively large insertion depths (corresponding to plasma electron temperatures of ~50 to 100 eV) and no macroscopic erosion, apart from removal of a thin oxide layer on their surface (Ref 113).

Plasma sprayed coatings were found to have higher deuterium retention than bulk tungsten (Ref 86), which might be a consequence of their porosity. On the other hand, deuterium permeation was found to be lower compared to bulk W (Ref 114). This was attributed mainly to the characteristic structural non-homogeneities of plasma sprayed coatings—voids and splat interfaces—possibly hindering diffusive transport due to different hydrogen diffusivities and solubilities in these regions compared to bulk material. Additionally, surface-connected pores could lead to re-emission on the upstream side. Studies at TEXTOR indicate that the main cause of deuterium retention on VPS tungsten layers is codeposition of deuterium with other impurities (carbon, boron) (Ref 115). Deuterium trapped in the components can be removed by transferred-arc cleaning (Ref 116).

PVD, CVD, and PS tungsten coatings are compared in Ref 25. PS is recommended for areas with smaller heat flux (below 5 MW/m^2), its advantages are high deposition rates and a better chance of in situ repair. CVD coatings have demonstrated thermal fatigue resistance up to 20 MW/m^2. Both PVD and CVD feature dense layers with high thermal conductivity, however, this does not necessarily translate to good thermal shock resistance. Also of concern with both the latter techniques are low deposition rates and high costs.

Other methods, such as electron beam evaporation, magnetron sputtering and arc deposition were considered in Ref 117, however, these can provide coatings in the μm range only.

3. Hydrogen Isotope Permeation Barriers

In a fusion reactor, the permeation of hydrogen isotopes (mainly tritium) through structural materials is an important issue because of its safety (radioactivity) and operational (fuel balance) implications (Ref 3, 118). This concerns the plasma facing components as well as the breeding blanket. In D-T fusion reactor systems, the breeding blanket is a necessary component, where tritium is produced from lithium by nuclear reaction with neutrons coming from the reactor core (Ref 1, 119). Two concepts are being investigated—solid breeder, based on lithium-containing ceramics, and liquid breeder, including lithium-containing metals (e.g., Pb-Li) and molten salts.

Since structural materials (e.g., steels) have very high hydrogen permeability (Ref 120), the permeation could be effectively reduced or hindered by thin surface layers from materials having low diffusivity and/or low surface recombination constants, thus acting as permeation barriers. Such coatings have to fulfill the following requirements (Ref 7, 119, 121):

- T-PRF > 1000 for a gas-phase permeation test and
- T-PRF > 100 for tests in liquid Pb-Li

where T-PRF is the tritium permeation reduction factor, compared to bare structural material (mainly reduced activation martensitic steel)

- Compatibility with Pb-Li, high corrosion resistance
- High thermomechanical integrity
- Self-healing (regeneration of the damaged barrier through in situ oxidation)
- Applicable to large engineering components

Moreover, these properties should be maintained at actual blanket operating conditions, which include a high radiation field, high temperature and its temporal and spatial gradients, high magnetic and electric fields and the presence of reactive liquid metals (Ref 119).

Materials with inherently low H permeability, such as oxides and intermetallics, are suitable (Ref 118). Al and Ti have high free energies of formation of their oxides, hence the ability to re-form even at low oxygen partial pressures (Ref 122). The barriers can be produced either by direct growth of oxide layers (Ref 121) or various coating techniques, such as hot-dip aluminizing (HDA), CVD, precipitation from liquid metals, ion implantation, cementation, chemical densification coating (CDC), or thermal spraying (Ref 7, 119, 121, 122).

Al was sprayed by VPS on MANET steel, followed by heat treatment (Ref 120), which induced interdiffusion and formation of Fe_3Al and Fe_2Al_5. The coatings were highly adherent, but brittle, containing cracks and delaminations. The permeation was tested using both deuterium (gas-phase), tritium (in Pb-Li) (Ref 121), resulting in T-PRF 100-1000 (depending on temperature), which was significantly better than other types of coatings. When the VPS Al coatings were subjected to post-oxidation (Ref 123), the T-PRF was about 500, independently of temperature. Similar coatings sprayed on steel tubes (Ref 124) exhibited slightly lower PRF than planar coatings (500 on F82H-mod and 44-117 on MANET in gas phase), but only 20 in Pb-17Li, possibly due to the wetting of the surface by the Pb-17Li and formation of $LiAlO_2$.

After preliminary and encouraging application of the detonation jet (DJ) spray of pure Al on MANET steel (Ref 125), the high temperatures necessary to transform completely the brittle Fe_2Al_5 into more ductile phases suggested the idea of a direct spraying of Fe-Al alloys. Ferritic-martensitic steels were coated with Fe(Cr, Al) solid solution layers (Ref 118), using HVOF, APS and VPS. However, the achieved T-PRF for the best coating (VPS) was 2.5 only, probably due to low adherence.

In Ref 7, the performance of several coatings produced by different techniques (HDA, CVD, VPS and DJ) was evaluated. Only the HDA and CVD coatings met the required gas-phase T-PRF > 1000, but failed to meet the T-PRF > 100 when exposed to Pb-Li. VPS coatings showed gas-phase T-PRF between 200 and 600 and Pb-Li T-PRF cca 30 (Ref 9, 124). Both the HDA and VPS coatings exhibited good corrosion resistance in Pb-Li. This is likely due to the high temperature treatment involved in the process, leading to the formation of protective alumina layer on the top surface (Ref 126).

In an overall evaluation of various tritium permeation barriers (Ref 122), it was concluded that the rate-controlling mechanism is the number and type of defects in the coatings. Most coatings are quite corrosion-resistant but their T-PRF degrades with neutron irradiation; important factor is the location of the coating (interior or exterior). The influence of substrate material was also observed (Ref 124).

Deuterium permeation barriers were also developed for SiC/SiC composites, proposed as low activation structural materials for the first wall (Ref 127). An A1-Si eutectic layer was plasma sprayed to SiC/SiC substrate and heat treated to maximize the interfacial bond strength. The alloy composition (11.2%Si) was chosen to promote wetting and to avoid brittle Al_4C_3 formation. SiC/SiC materials have many diffusion paths due to interconnected porosity and are much more permeable than non-porous coatings; the coatings' barrier function is apparently fulfilled by blocking the pores in the SiC/SiC surface region.

A duplex coating system consisting of 0.1 mm Ta bondcoat and 0.5 mm Cr_2O_3 topcoat has been plasma sprayed on a Ti alloy substrate, which is also among the candidate structural materials (Ref 128). Low activation of the components was one of the main requirements for the selection of the coating system. In hydrogen charging tests, no penetration through the coated sample was observed, demonstrating its barrier efficiency.

The uptake, permeation, retention, and release of hydrogen isotopes is also an important issue for PFM, as it affects working gas recycling, plasma behavior and tritium inventory (Ref 114, 129, 130). The relevant properties of some of these materials were mentioned in the previous section.

4. Electrical Insulation

For self-cooled liquid metal blankets in tokamaks with high magnetic fields, where the liquid serves both as a breeder and a coolant, electrically insulating coatings are necessary (Ref 131). Otherwise, the magnetic field acting on flowing metal would induce electrical currents if the potential drop is short-circuited by the ducts. The resulting magnetohydrodynamic drop, in turn, would impart large mechanical stresses on the duct walls. In this application, the coatings would have to provide electrical insulation, in addition to the requirements mentioned in the beginning of previous section (mainly compatibility with liquid Li). The product of resistivity and thickness should be $> 100\ \Omega \cdot cm^2$ (Ref 7). However, electrically insulating coatings find application in other locations as well.

For the insulating coatings for liquid metal blankets, oxides and nitrides are the prime candidates (Ref 7, 131). The production techniques include in situ formation during exposure of V alloys to lithium with controlled chemistry, various vapor deposition processes (Ref 7), pre-aluminization of the substrate followed by oxidation or nitridation (Ref 131), and plasma spraying (Ref 132). An important challenge is posed by irradiation effects on ceramics—reduction in strength, thermal conductivity, and electrical degradation (Ref 131, 133).

Plasma sprayed Y_2O_3 with pores filled by chemical densification (Ref 132) showed good electrical resistance (10^8-$10^{11}\ \Omega \cdot cm$ in the foreseen application temperature range, 200-800 °C) (Ref 134), but insufficient compatibility with liquid lithium. While sintered Y_2O_3 performed well, plasma sprayed coating delaminated (Ref 132). Lithium penetrated into the coating layer through small cracks and reacted on Y_2O_3 to form $LiYO_2$, which has a different density from that of Y_2O_3 and is more brittle than Y_2O_3. It was concluded that Y_2O_3 has a potential as a ceramic coating material for liquid blankets if it can be made into a dense coating.

$MgO \cdot Al_2O_3$ is another candidate for liquid blanket insulator, having high electrical resistivity and radiation resistivity. It was applied by APS on a stainless steel interlayer (prepared by VPS or APS), followed by densification (impregnation by a $(YNO_3)_3$ solution and firing) to close open pores (Ref 135).

The thermal shock resistance of the coatings was best at an optimum surface roughness of the SS interlayer—increasing roughness improved adhesion up to a certain point, above which it was too high and caused selective delamination of uneven top coating. While the porosity was comparable to sintered ceramic, the thermal conductivity was less than 50% (Ref 136).

Al_2O_3, which also features high electrical and radiation resistivity, was applied by APS over VPS stainless steel and APS Ni-20Cr bondcoats (Ref 137). These coatings exhibited sufficient thermal shock resistance as well as electrical resistivity ($> 10^{13}\ \Omega \cdot cm$ at RT, decreasing with increasing temperature). Better thermal shock performance of the coatings with SS interlayer was attributed to relaxation of thermal stress because of higher porosity of the bondcoat. In mechanical impact tests, simulating the loads due to electromagnetic forces during a disruption, no change in electrical resistivity or integrity was observed.

Plasma sprayed spinel is being considered as a candidate material for the insulator rings of the ITER neutral beam injector bushing (Ref 138). These insulators will have to stand high voltages (of the order of 1 MV), face high vacuum on one side and pressurized gas on the other, and will be subject to a radiation field from the plasma and the accelerator itself. Electrical degradation studies (Ref 138) showed very low radiation induced conductivity even at high radiation doses, but serious surface electrical degradation at higher temperatures (above 150 °C), even without radiation.

For the electrical insulation for the stainless steel, Inconel and bronze components of the ITER vessel, plasma sprayed alumina is planned (Ref 139). Coatings of 500 μm thickness provide electrical insulation of 1 kV and have shown good thermal shock resistance, high impact strength and load capability up to the yielding of the carrier. Plasma sprayed alumina is also foreseen for electrical insulation of the remote handling system for ITER blanket modules (Ref 140); tests have indicated satisfactory insulating and mechanical properties as well as thermal cycling behavior.

5. Joining and Other Applications

5.1 Bondcoats and the Use of Spraying for Joining

As multiple materials combinations are being used or planned for fusion-oriented devices, joining is an important issue. In particular, this concerns the plasma facing layers bonded to either structural materials or the cooling system. A number of joining techniques are being investigated which include silverless brazing, diffusion bonding, hot isostatic press (HIP) bonding, explosive bonding and plasma spraying (Ref 79, 141). The main issues are the largely different thermal and mechanical properties and resulting stress concentration at the interface (e.g., W/Cu, W/C, C/Cu) and possible formation of brittle compounds upon exposure to high temperatures, either during fabrication or in service (mainly Be/Cu, also W/C). These issues, too, can be addressed by applying plasma sprayed coatings.

Joining beryllium directly to copper presents a challenging problem due to the formation of brittle intermetallic compounds, such as BeCu, Be_2Cu, at the interface. Plasma sprayed vanadium, intended to serve as a diffusion barrier (Ref 79), did not provide enough strength and led to layer separation. When plasma sprayed aluminum was used as a diffusion barrier (Ref 141), depending on subsequent bonding parameters, fracture strength of such joints was better or comparable to a PVD alternative, reaching even 100% of bulk aluminum value (Ref 142).

For joining solid W rods to Cu heat sink, plasma spraying is among the methods considered for pre-coating the rod tips before diffusion bonding or hipping the assembly (Ref 141). Medium scale mock-ups with such

tungsten ''macrobrush'' armor, 3 mm plasma sprayed OFHC copper interlayer, electron beam welded or hipped to CuCrZr heat sink, were successfully tested under heat fluxes around 20 MW/m^2 (Ref 143).

Functionally graded materials (FGMs) are able to reduce the thermal stresses and increase the lifetime by suitable choice of the composition of the graded layer; this has been demonstrated by numerical simulations (Ref 144-146). Plasma spraying can be used to produce a graded layer that may serve either as a stress reliever between the plasma facing layer and the heat sink, or encompass the plasma facing surface as well, thus eliminating the need for further joining.

In Ref 147, W-Cu FGM by PS and laser sintering (LS) were studied. Both methods offer good possibilities to produce W-Cu graded layers. However, production of a full FGM by LS was only possible when starting from the Cu end (otherwise, the copper would either evaporate or the tungsten would not melt sufficiently). The plasma sprayed composite had mechanical properties comparable to commercially produced solid composite [formed by copper infiltration of porous tungsten (Ref 49)] and lower thermal conductivity.

In Ref 148, W/Cu composites and graded layers were produced by VPS, using three types of powders—Cu-coated W (40 vol.% W), pre-mixed (75 vol.% W) and separate powders, mixed at the point of injection (64 vol.% W). Coatings of the first type contained less W than feedstock, likely due to bouncing of unmolten W particles, but very low porosity. Coatings from the pre-mixed powder, on the other hand, had decreased content of Cu (due to Cu overheating, as the plasma jet had high enough enthalpy to melt the tungsten), and porosity about 8%. The best results were obtained with separate powders (porosity ~3%). In all cases, transferred arc cleaning applied during spraying resulted in densification of the coating and only minor changes in composition. Graded layers were produced using the individual powders. Porosity varied from <1% on the Cu end to ~7% on the W end, while thermal conductivity was higher than of the uniform composite.

In Ref 149, W + Cu composites and FGMs were produced by LPPS and WSP; this was followed by a heat treatment in reducing atmosphere (H_2) for densification and removal of oxides. Young's modulus, thermal expansion, and thermal diffusivity were determined as a function of composition. Generally, the mechanical properties were close to copper, while the thermal conductivity was lower than both bulk copper and tungsten. Interesting behavior of thermal conductivity vs. temperature was found. For the Cu-rich composites, the conductivity was the lowest at room temperature, but highest at higher temperatures (above 400 °C). This was attributed to thermal expansion and filling of the voids at higher temperatures. The measured properties served as input for FEM calculations to optimize the compositional profile. Stress profile calculations at 500 °C confirmed the reduction of stress at the interface when FGM is used as an interlayer, instead of a sharp interface between bulk W and Cu. The stress magnitude and location of the maximum were dependent not only on the compositional profile, but also on the compound size (Ref 150).

In Ref 151, a thin film copper bondcoat is proposed to promote bonding of plasma sprayed W + Cu FGM to bulk tungsten, while the bonding to bulk copper on the other side can be achieved by low temperature HIPping.

Nickel-based interlayers, graded with tungsten, were also used to enhance the bonding of plasma sprayed W to Cu-based substrate; however, nickel has high activation due to neutron flux and thus its content has to be very limited (Ref 152). For components made of low activation steel or stainless steel, mixed tungsten/steel interlayers were applied to reduce the residual and thermal stresses at the substrate-coating interface and to improve the adhesion of the coating. The advantage of this mixed interlayer is that no further (high activation) materials need to be introduced to improve coating adhesion. Heat load tests confirmed the thermomechanical suitability of these coatings for plasma facing first wall components made of steel (Ref 93).

5.2 Other Applications

Coatings have also been developed for the first wall of an inertial confinement fusion reactor. The materials requirements are to some extent similar to magnetic confinement fusion, as listed in Section 2. Additionally, the coatings must be able to survive the target explosion (impact of debris, ions, scattered laser light and especially x-rays), should have low erosion from CO_2 cleaning, low vacuum outgassing, low activation by neutrons and be compatible with the target materials (Ref 90, 153, 154). In service, the coating would be subject to frequent thermal shocks of minor amplitude (<50 °C) due to target explosions, and infrequent but more severe thermal cycles (~475 °C) due to startup and shutdown (Ref 154). During the target explosions, the vessel surface temperature can easily reach the melting point of high-Z materials, therefore the size of the vessel has to be large enough to avoid any melting of the wall.

Tantalum was chosen among various candidate materials for its favorable mechanical and chemical properties, relatively high melting point, as well as good fabricability and low cost. 1 mm plasma sprayed Ta coatings on ferritic steel were tested under thermal cycling (Ref 154). The coatings survived 100 cycles of 465 °C amplitude without cracking or delamination. Other observations indicated the coatings to be brittle, probably due to oxygen and nitrogen contamination (oxides and nitrides detected by XRD and SEM).

Another candidate material is B_4C. In Ref 153, plasma sprayed B_4C, $MgAl_2O_4$, Al_2O_3 and their composites were studied. Graded bond layers were applied to mitigate the thermal mismatch with high CTE aluminum substrates. A number of application-relevant properties were investigated; in different tests different coatings ranked the best. In Ref 61, the spraying conditions were optimized for low porosity, to reduce outgassing. Higher particle temperatures were achieved with higher H_2 content in the plasma gas, resulting in porosities below 5%. APS B_4C coatings exhibited higher resistance to laser pulses than other

studied materials (carbon-based), but significantly higher outgassing compared to bulk materials.

B_4C, sprayed by WSP has shown interesting electrical properties—namely, significant RF wave absorption (Ref 155) that makes them suitable, e.g., for electron cyclotron heating waveguides. A variation of the power reflection coefficient (R) between 0.15 and 0.82, depending on spraying parameters, was found. Even higher absorption (R as low as 0.03) was found in a duplex layer, consisting of plasma sprayed alumina covered by colloidal graphite. The electrical conductivity of B_4C, being between a conductor and an insulator, proved advantageous for the protective coating of a Langmuir probe, used for 2-D measurements of plasma density and potentials in a tokamak; this probe was successfully applied in tokamak CASTOR (Ref 156).

6. Materials Testing

Besides standard characterization techniques applied to thermal spray coatings, there are specific tests that follow from the requirements for application in fusion environments. The performance of certain coatings in some of these tests was already mentioned in previous sections.

6.1 High Heat Flux Testing

The simulation of fusion relevant heat fluxes to PFM must cover both, normal operation conditions and transient events such as plasma disruptions, VDEs and Edge Localized Modes (so-called type-I ELMs), (cf. Table 1). Normal operation conditions on actively cooled components are mainly performed in electron or ion beam test facilities (Ref 157-159). Electron beam devices use focused beams with diameters ranging from typically 1 to 10 mm; to provide homogeneous thermal loads to the full surface of the module and to control the pattern size and shape, fast beam scanning modes (e.g., saw tooth-filled, triangular-filled rectangles or TV-raster scans with flyback) are applied. Typical electron energies are 30-200 keV; hence, electron beam loading is associated with a volumetric heating of the beam affected surface layer. The typical penetration depth ranges from a few microns in high-Z materials such as tungsten to several hundred microns in low materials (B_4C or beryllium). This has to be taken into consideration when HHF methods are applied to thin coatings.

Ion beam test devices (Ref 160) use hydrogen, deuterium, or helium beams with typical particle energies of 50 keV; here a true surface heating can be simulated. In comparison to electron beam devices the beam diameters range from 7 to 20 cm with Gaussian shaped beam profiles. To cover larger surface areas, a flat angle of incidence or multiple beam systems are applied. High-performance HHF test today provide electron beam powers from several ten to > 1000 kW; ion beam devices are operated in the MW-range up to 7.5 MW.

The heat removal efficiency of actively cooled components is investigated in long-pulse load tests with quasi-stationary pulses to guarantee thermally stationary conditions. The applied power densities are increased stepwise to determine the failure limits of the test modules. In so-called thermal fatigue tests high cycle numbers (1000-5000 cycles) at a predetermined power density level are applied periodically; representative cycle durations are 20-60 s.

Due to the limited heat fluxes in the first wall region, tests on primary wall modules can also be performed in IR-test facilities, in particular if high cycle number have to be achieved. The maximum power density in IR devices remains below 1 MW/m^2 (Ref 161).

Transient thermal loads with power densities in the GW/m^2-range cannot be applied in ion beam test facilities; here the electron beam devices outclass most other test devices due to their capability to focus the beam and to scan it with very high raster frequencies to provide homogeneous load patterns on small surface areas. In addition, pulsed laser devices were used to simulate disruptions, with 0.2-20 ms durations and energy densities are up to 10 MJ/m^2 (Ref 162, 163); plasma accelerators (Ref 164) and high-power ion accelerators (Ref 165) are being used to simulate very short transient events in the sub-millisecond (ELMs) or even in the sub-microsecond-range (simulation of inertial confinement regimes). Up to now the repletion rate in those test devices is limited to several hundred or at best a few thousand pulses. Inertial confinement studies and ELM simulation tests, however, require pulse numbers $\geq 10^6$ pulses. Here e-beam test facilities with flexible beam scanning generators are the promising candidate.

To quantify the response of plasma facing components to intense thermal loads a number of diagnostics has been developed and adapted. These include among others a careful thermal characterization using calorimeters to quantify the absorbed energy by the test specimens and/or coolant water calorimetry based on delta T and flow rate; in addition, beam profile measurements and records of the absorbed beam current are applied. Surface temperature distributions and bulk temperatures are determined by high resolution infrared cameras, pyrometers, and thermo couples. For the in situ analysis of the thermally induced material erosion high resolution imaging techniques are used (droplet formation, melt layer motion, and brittle destruction, Ref 166). The formation of thermally induced cracks during intense thermal shocks can also be traced by acoustic emission techniques.

6.2 Infrared Inspection of Coatings

Besides electron beam testing, an equivalent diagnostic techniques, namely non-destructive testing by infrared methods are routinely applied. This method is based on a careful diagnosis of the temperature distribution of the plasma facing surface under coinstantaneous streams of cold and hot water in the coolant tubes. Any defect in the joining interface can be clearly detected by a sensitive IR camera from a delayed temperature adjustment of defective armour tiles. Another technique, the so-called lock-in thermography is based on an external sinusoidal thermal excitation generated by a set of modulated flash-lamps.

The phase-shift of the recorded infrared signal depends on the presence of cracks or other defects in the interface layer of the component (Ref 167, 168). These methods have also been successfully applied to plasma sprayed coatings on metallic substrates to detect detachments form the substrate and delamination processes inside the coating (Ref 50).

6.3 Tritium Permeation Testing

Hydrogen permeation barrier coatings are typically tested in two steps—in the gas phase and in liquid Pb-Li.

In the gas-phase test, one side of the sample is exposed to hydrogen or deuterium gas at a known, fixed pressure. The gas permeating through the sample is released at the other side, where it causes a pressure rise in an initially evacuated, calibrated volume. The pressure rise is measured using a manometer. Since the volume is calibrated, the rate of pressure rise could be converted into an amount of gas permeating through unit area of the sample per second (Ref 120). The high pressure gas and the permeated gas can be analyzed with a mass spectrometer, to check for possible contaminants and to distinguish permeation from outgassing. The permeability of the coated sample at a given temperature is then compared to that of an uncoated base material and the permeation reduction factor (T-PRF) is determined. In an alternative arrangement, deuterium can be implanted on one side by an ion beam (Ref 114). In hydrogen charging experiments, the samples are attached to a vacuum chamber, which is then filled with a controlled amount of hydrogen gas. The chamber pressure evolution with time is monitored and its decrease is correlated with hydrogen penetration through the sample (Ref 128).

In the second type of test, either the coated or the uncoated side of the sample is immersed in the molten alloy (Ref 124). The tritium released on the other side is mixed with a He purge gas that carries it to tritium monitoring systems consisting of ionization chambers and water bubbler traps (Ref 119). Additionally, long-term exposures of the coatings to liquid Li alloys are carried out to test their compatibility/corrosion resistance (Ref 126).

7. Conclusions

The materials to be applied in a fusion reactor will be subject to extreme and complex loading conditions and have to fulfill very complex and sometimes contradicting requirements (for example, high Z/low Z for plasma facing components). The materials selection is further complicated by the fact that many of the processes taking place during reactor operation can only be quantified by making largely simplifying assumptions. The interaction between the knowledge in plasma physics, process control, materials selection and development is continually evolving.

A number of the demands on fusion materials can be fulfilled by the application of coatings. Thermal spraying is just one of the available coating technologies. Its advantages are the following:

- A single-step manufacturing technology, without the need for further joining
- Coatings can be applied without significant substrate heating, thus without changing the substrate microstructure or strength
- Possibility of coating large areas even of non-planar shapes
- Ability to produce thick coatings, of the order of mm
- Ability to produce FGMs easily, thus reducing the stress concentration at the interface
- Easy repairing
- Low cost production
- High strain tolerance due to porosity and lamellar structure.

Its disadvantages include:

- Structural defects (porosity, cracks), resulting in low thermal conductivity, chemical attack on the substrate, prolonged impurity release to the plasma, etc.
- Impurities. Generally, plasma spraying in vacuum (VPS) or in controlled atmosphere (CAPS) is superior to atmospheric plasma spraying in both these aspects. However, the use of vacuum chamber poses serious limitations on coated component size and shape, besides increased cost.

Thermal spray (especially plasma spray) coatings were developed and tested for a variety of applications in fusion environments, including plasma facing components, tritium permeation barriers and electrical insulation. During the development, some of the concepts or materials combinations were discarded, some were qualified for application or are currently applied, while some are considered as alternative approaches. In the area of plasma facing components, for example, plasma sprayed B_4C coatings are applied in several locations in Tore Supra tokamak (Ref 169) and are qualified as a coverage of the first wall of Wendelstein 7-X stellarator (Ref 54). Plasma sprayed W coatings are candidates for divertor components (ITER and DEMO) receiving moderate heat loads (Ref 93). Plasma sprayed ceramic materials were selected for electrical insulation of certain vacuum vessel components for ITER (Ref 139). For the combined insulation and tritium permeation barrier application, a number of competing technologies are available, some of which provide similar results at lower costs (Ref 170).

In conclusion, plasma spraying is a prospective technology for certain fusion applications, while the development in some areas is still ongoing.

Acknowledgments

The research and development of plasma sprayed B4C and W coatings for fusion applications was supported in part by EFDA Task DV4/04 (TW0) in 2000 and EFDA Task TW5-TVM-PSW in 2005, respectively.

References

1. J. Ongena and G. VanOost, Energy for Future Centuries: Will Fusion be an Inexhaustible, Safe, Clean Energy Source?. *Trans. Fusion Technol.* 2000, **37**, p 3-15
2. D.J. Campbell, The ITER Project. 20th Symposium on Plasma Physics and Technology, (Prague), 2002
3. ITER, http://www.iter.org
4. H.P. Furth, Nuclear Fusion - Power Source of the Future? *Britannica Yearbook Sci Future*, 1974, p 111-127
5. Lawson's criterion, http://en.wikipedia.org/wiki/Lawson_criterion
6. C.C. Baker, Advances in Fusion Technology. *J. Nucl. Mater.*, 2000, **283**, p 1-9
7. D.L Smith., J. Konys, T. Muroga, and V. Evitkhin, Development of Coatings for Fusion Power Applications. *J. Nucl. Mater.*, 2002, **307**, p 1314-1322
8. H. Bolt, V. Barabash, G. Federici, J. Linke, A. Loarte, J. Roth, and K. Sato, Plasma Facing and High Heat Flux Materials – Needs for ITER and Beyond. *J. Nucl. Mater.*, 2002, **307**, p 43-52
9. D.L. Smith, J.H. Park, I. Lyublinski, V. Evtikhin, A. Perujo, H. Glassbrenner, T. Terai, and S. Zinkle, Progress in Coating Development for Fusion Systems. *Fus. Eng. Des.*, 2002, **61-62**, p 629-641
10. R.K. Janev and A. Miyahara, Plasma Material Interaction Issues in Fusion-Reactor Design and Status of the Database. *Nucl. Fusion*, 1991, **1**, p 123-138
11. J. Linke, H. Bolt, and M. Roedig, Material Aspects for Plasma Facing Components in Thermonuclear Fusion Reactors, *Proc. 5th Eur. Conf. on Advanced Materials, Processes and Applications,* (Maastricht, Netherlands), 1997, p 419-422
12. R. Matera and B. Federici, Design Requirements for Plasma Facing Materials in ITER. *J. Nucl. Mater.*, 1996, **237**, p 17-25
13. A. Hassanein and I. Konkashbaev, Theory and Models of Material Erosion and Lifetime During Plasma Instabilities in a Tokamak Environment. *Fus. Eng. Des.*, 2000, **51-52**, p 681-694
14. K. Ehrlich, M. Gasparotto, L. Giancarli, G. Le Marois, S. Malang, and B. van der Schaaf, European Materials Assessment Meeting, Report EFDA-T-RE-2.0, EFDA, Garching, Germany, 2002
15. R.W. Conn, R.P. Doerner, and J. Won, Beryllium as the Plasma-Facing Material in Fusion Energy Systems - Experiments, Evaluation, and Comparison With Alternative Materials, Fus. *Eng. Des.*, 1997, **37**(4), p 481-513
16. K. Tokunaga, N. Yoshida, N. Noda, T. Sogabe, and T. Kato, High Heat Load Properties of Tungsten Coated Carbon Materials. *J. Nucl. Mater.*, 1998, **263**, p 998-1004
17. J.W. Davis, V.R. Barabash, A. Makhankov, L. Plochl, and K.T. Slattery, Assessment of Tungsten for Use in the ITER Plasma Facing Components. *J. Nucl. Mater.*, 1998, **263**, p 308-312
18. R. Aymar, ITER Status, Design and Material Objectives. *J. Nucl. Mater.*, 2002, **307-311**(1), p 1-9
19. J. Wesson, Tokamaks. Oxford University Press, New York, 2004
20. V. Gutzeit, H. Hoven, J. Linke, and M. Rödig, Examination of Material Damage on Components of Future Fusion Reactors. *Prakt. Metallogr.*, 1998, **35**(3), p 136-147
21. M. Merola, M. Akiba, V. Barabash, and I. Mazul, Overview on Fabrication and Joining of Plasma Facing and High Heat Flux Materials for ITER. *J. Nucl. Mater.*, 2002, **307**, p 1524-1532
22. V. Barabash, M. Akiba, I. Mazul, M. Ulrickson, and G. Vieider, Selection, Development and Characterisation of Plasma Facing Materials for ITER. *J. Nucl. Mater.*, 1996, **237**, p 718-723
23. F. Thevenot, Boron Carbide - A Comprehensive Review. *J. Eur. Ceram. Soc.*, 1990, **6**, p 205-225
24. D.J. Varacalle and R.G. Castro, Analysis of the Plasma-Particle Interaction During the Plasma Spraying of Beryllium. *J. Nucl. Mater.*, 1996, **230**(3), p 242-246
25. I. Smid, M. Akiba, G. Vieider, and L. Plochl, Development of Tungsten Armor and Bonding to Copper for Plasma- Interactive Components. *J. Nucl. Mater.*, 1998, **263**, p 160-172
26. S. Janisson, A. Vardelle, P. Fauchais, and E. Meillot Correlation between the Properties of Plasma-Sprayed Boron Carbide Coatings and Particle Parameters at Impact, *Proc. 14th intl. Symp. on Plasma Chemistry,* (Prague, CZ) 1999, p 2049-2056
27. F. Březina, J. Mollin, R. Pastorek, and Z. Šindelář, Chemické tabulky anorganických sloučenin (Chemical Tables of Inorganic Substances). SNTL, Praha, 1986 (in Czech)
28. M. Semchysen Refractory Metals and Alloys. In M.B. M.B. Bever (Ed.*Encyclopedia of Materials Science and Engineering* (pp. 4159-4161). Oxford: Pergamon Press, 1986
29. Gmelin Handbook, Gmelin Institut fuer Anorganische Chemie und Grenzgebiete and Beilstein Informationssysteme GmbH, 1998
30. MatWeb, http://www.matweb.com
31. S. Deschka, J. Linke, H. Nickel, and E. Wallura, Performance of Plasma Sprayed Boron Carbide Coatings under High Heat Loads. *Fus. Eng. Des.*, 1991, **18**, p 157-162
32. C.J. Smithells, Metals Reference Book (4th ed.). Butterworths, London, 1967
33. Web Elements, http://www.webelements.com
34. M. Isobe, Y. Ohtsuka, H. Shinonaga, Y. Ueda, B. Kyoh, and M. Nishikawa, Erosion Yield of Graphite and B4C Irradiated by High-Flux Deuterium Beams. *Fus. Eng. Des.*, 1995, **28**, p 170-175
35. A to Z of Materials, http://www.azom.com
36. M. Wahba, On The Use of Beryllium as Thermal Neutron Filter. *Egypt. J. Sol.*, 2002, **25**(2), p 215-227
37. P.J. Karditsas and M.-J. Baptiste, Thermal and Structural Properties of Fusion Related Materials, http://aries.ucsd.edu/LIB/PROPS/PANOS/matintro.html
38. F. Brossa, G. Rigon, and B. Looman, Behavior of Plasma Spray Coatings Under Disruption Simulation. *J. Nucl. Mater.*, 1988, **155**, p 267-272
39. P. Groot, J.G. Vanderlaan, M. Mack, M. Dvorak, and P. Huber, Plasma-Sprayed Titanium Carbide Coatings for 1st-Wall Applications in Fusion Devices. *J. Nucl. Mater.*, 1991, **179**, p 370-374
40. R.G. Saintjacques, F. Bordeaux, B. Stansfield, G. Veilleux, W.W. Zuzak, A. Lakhsasi, C. Boucher, and C. Moreau, Enhanced Resistance of Plasma-Sprayed TiC Coatings to Thermal Shocks. *J. Nucl. Mater.*, 1992, **191**, p 465-468
41. M. Ducos and E. Gauthier, Plasma Sprayed B4C Coatings in Controlled Fusion Reactors. *Surf. Eng.*, 1993, **9**(2), p 134-136
42. M. Lipa and E. Gauthier, Characterization of Boron Carbide Coatings for Actively Cooled Plasma Facing Components, *Proceedings of the 18th Symposium on Fusion Technology*, K. Herschbach, W. Maurer, and J.E. Vetter, Ed., Elsevier, 1995, p 455-458
43. J.G. van der Laan, G. Schnedecker, E.V. van Osch, R. Duwe, and J. Linke, Plasma-Sprayed Boron-Carbide Coatings for 1st-wall Protection. *J. Nucl. Mater.*, 1994, **211**(2), p 135-140
44. W. Mallener, D. Stoever, Plasma Spraying of Boron Carbide Using Pressures up to Two Bar, *Thermal Spray Coatings: Research, Design and Applications*, C.C. Berndt and T.F. Bernecki, Ed., June 7-11, 1993 (Anaheim, CA), ASM International, 1993, p 291-295
45. W. Mallener, H.J. Gross, and D. Stoever, Properties of Plasma Sprayed Boron Carbide Coatings, *Thermal Spray Industrial Applications*, C.C. Berndt and S. Sampath, Ed., June 20-24, 1994 (Boston, MA), ASM International, 1994, p 627-632
46. H. Bolt, M. Araki, J. Linke, W. Mallener, K. Nakamura, R.W. Steinbrech, and S. Suzuki, Heat Flux Experiments on First Wall Mock-Ups Coated by Plasma Sprayed B4C. *J. Nucl. Mater.*, 1996, **237**, p 809-813
47. A. Riccardi and A. Pizzuto, Thermomechanical Characterization of B4C Vacuum Plasma Sprayed Coatings on Stainless Steel Tubular Substrates. *J. Mater. Sci. Lett.*, 1996, **15**(14), p 1234-1236
48. Y. Zeng, J.W. Feng, and C.X Ding, Microstructure and Properties of Plasma Spraying Boron Carbide Coating. *J. Mater. Sci. Technol.*, 2000, **16**(1), p 63-66
49. C.C. Ge, J.T. Li, Z.J. Zhou, W.B. Cao, W.P. Shen, M.X. Wang, N.M. Zhang, X. Liu, and Z.Y. Xu, Development of Functionally Graded Plasma-Facing Materials. *J. Nucl. Mater.*, 2000, **283**, p 1116-1120

50. P. Chappuis, F. Escourbiac, M. Chantant, M. Febvre, M. Grattarola, M. Bet, M. Merola, and B. Riccardi, Infrared Characterization and High Heat Flux Testing of Plasma Sprayed Layers. *J. Nucl. Mater.*, 2000, **283**, p 1081-1084
51. J. Matějíček, K. Neufuss, P. Ctibor, P. Rohan, J. Dubský, P. Chráska, and V. Brožek, WSP-Sprayed Boron Carbide Coatings for Fusion Applications, *International Thermal Spray Conference*, E. Lugscheider and C.C. Berndt, Ed., March 4-6, 2002 (Essen, Germany), DVS Deutscher Verband für Schweißen, 2002, p 1-5
52. D. Valenza, H. Greuner, G. Hofmann, S. Kotterl, J. Roth, and H. Bolt, Characterisation and Thermal Loading of Low-Z Coatings for the First Wall of W7-X. *J. Nucl. Mater.*, 2002, **307**, p 89-94
53. J.E. Doring, R. Vassen, J. Linke, and D. Stover, Properties of Plasma Sprayed Boron Carbide Protective Coatings for the First Wall in Fusion Experiments. *J. Nucl. Mater.*, 2002, **307**, p 121-125
54. H. Greuner, M. Balden, B. Boeswirth, H. Bolt, R. Gadow, P. Grigull, G. Hofmann, T. Huber, W. Kasparek, and H. Kumric, Evaluation of Vacuum Plasma-Sprayed Boron Carbide Protection for the Stainless Steel First Wall of WENDELSTEIN 7-X. *J. Nucl. Mater.*, 2004, **329-333**(1), p 849-854
55. S. Deschka, C. Garciarosales, W. Hohenauer, R. Duwe, E. Gauthier, J. Linke, M. Lochter, W. Mallener, L. Plochl, P. Rodhammer, and A. Salito, Manufacturing and High Heat Flux Loading of Tungsten Coatings on Fine Grain Graphite for the ASDEX-Upgrade Divertor. *J. Nucl. Mater.*, 1996, **237**, p 645-649
56. H.D. Steffens, M. Dvorak, and P. Groot, Thermal-Behavior of Thick TiC Layers Made by Plasma Spraying. *Surf. Coat. Technol.*, 1991, **49**(1-3), p 46-49
57. H. Bolt, Nonmetallic Materials for Plasma Facing and Structural Applications in Fusion-Reactors, Fus. *Eng. Des.*, 1993, **22**(1-2), p 85-98
58. O.I. Buzhinskij and Y.M. Semenets, Thick Boron Carbide Coatings for Protection of Tokamak First Wall and Divertor. *Fus. Eng. Des.*, 1999, **45**(4), p 343-360
59. M. Laux, W. Schneider, P. Wienhold, B. Juttner, A. Huber, M. Balden, J. Linke, H. Kostial, M. Mayer, M. Rubel, A. Herrmann, A. Pospieszczyk, S. Jachmich, B. Schweer, D. Hildebrandt, and H. Bolt, Arcing at B4C-Covered Limiters Exposed to a Sol-Plasma. *J. Nucl. Mater.*, 2003, **313**, p 62-66
60. L. Bianchi, P. Brelivet, A. Freslon, A. Fornier, C. Cordillot, F. Jequier, and D. Schirmann, Plasma Sprayed Boron Carbide Coatings as First Wall Material for Laser Fusion Target Chamber, *Thermal Spray: Meeting the Challenges of the 21st Century*, C. Coddet, Ed., May 25-29, 1998 (Nice, France), ASM International, 1998, p 945-950
61. V.A. Lavrenko, A.P. Pomytkin, P.S. Kislyj, and B.L. Grabchuk, Kinetics of High Temperature Oxidation of Boron Carbide in Oxygen. *Oxid. Met.*, 1976, **10**(2), p 85-95
62. V. Brozek, J. Dubsky, B. Kolman, K. Neufuss, and P. Chraska, Plasma Sprayed Coatings of Borides, Carbides and Silicide, *Proc. AustCeram 92*, Melbourne, 1992, p 777-786
63. H. Gruhn, W. Fischer, C. Funke, W. Malléner, D. Stöver, Residual Stress Calculation by Finite Element Methods, *Thermal Spray: Practical Solutions for Engineering Problems*, C.C. Berndt, Ed., Oct 7-11, 1996 (Cincinnati, OH), ASM International, 1996, p 869-874
64. W. Mallener, H. Gruhn, and H. Hoven, Plasma-Sprayed High- and Low-Z Materials for the Protection of Inner Walls in Nuclear Fusion Devices, *Thermal Spraying: Current Status and Future Trends*, A. Ohmori, Ed., May 22-26, 1995 (Kobe, Japan), High Temperature Society of Japan, 1995, p 229-233
65. J. Linke, H. Bolt, R. Doerner, H. Grubmeier, Y. Hirooka, H. Hoven, C. Mingam, H. Schulze, M. Seki, E. Wallura, T. Weber, and J. Winter, Performance of Boron Carbon 1st Wall Materials Under Fusion Relevant Conditions. *J. Nucl. Mater.*, 1990, **176**, p 856-863
66. J. Linke, M. Akiba, H. Bolt, J. Vanderlaan, H. Nickel, E. Vanosch, S. Suzuki, and E. Wallura, Simulation of Disruptions on Coatings and Bulk Materials. *J. Nucl. Mater.*, 1992, **196**, p 607-611
67. J.N. Yu, Z.W. Yao, G. Yu, F.M. Chu, X.Z. Tang, Y. Zeng, and T. Noda, The Behavior of Coatings and SiCf/SiC Composites Under Thermal Shock. *J. Nucl. Mater.*, 2000, **283**, p 1077-1080
68. K. Nakamura, M. Akiba, M. Araki, M. Dairaku, K. Sato, S. Suzuki, K. Yokoyama, T. Ando, R. Jimbou, M. Saidoh, K. Fukaya, H. Bolt, and J. Linke, Thermal Tests on B4C-Overlaid Carbon-Fiber-Reinforced Composites Under Disruption Heat Load Conditions. *Fus. Eng. Des.*, 1995, **30**(3), p 291-298
69. C. Fuentes, M. Blaumoser, J. Botija, D. Ciric, J. Guasp, M. Liniers, A. Salito, and B. Schedler, Development and Tests of B4C-Covered Heat Shields for TJ-II. *Fus. Eng. Des.*, 2001, **56-57**, p 315-319
70. J.P. Coad, B. Farmery, J. Linke, and E. Wallura, Experience With Boron-Carbide Coated Target Tiles in Jet. *J. Nucl. Mater.*, 1993, **200**(3), p 389-394
71. H. Bolt, R. Duwe, V. Philipps, A. Pospieszczyk, B.B. Schweer, B.B. Unterberg, and E. Wallura, Behaviour of Boron-Carbide Materials in TEXTOR and Under Electron Beam Irradiation, *J. Nucl. Mater.,* 1994, **212-215**(pt. B), p 1239-1244
72. R. Jimbou, K. Kodama, M. Saidoh, Y. Suzuki, M. Nakagawa, K. Morita, and B. Tsuchiya, Thermal Conductivity and Retention Characteristics of Composites Made of Boron Carbide and Carbon Fibers with Extremely High Thermal Conductivity for First Wall Armour. *J. Nucl. Mater.*, 1997, **241-243**, p 1175-1179
73. A Yehia, R. Vassen, R. Duwe, and D. Stover, Ceramic SiC/B4C/TiC/C Composites as Plasma Facing Components for Fusion Reactors. *J. Nucl. Mater.*, 1996, **237**, p 1266-1270
74. P.G. Valentine, P.W. Trester, J. Winter, J. Linke, J.L. Kaae, A. Schuster, H. Bolt, R. Duwe, E. Wallura, and V. Philipps, B4C-SiC Reaction Sintered Coatings on Graphite for Plasma-Facing Components. *J. Nucl. Mater.*, 1995, **220-222**, p 756-761
75. O.I. Buzhinskij, V.A. Barsuk, I.V. Opimach, V.G. Otrozhenko, A.I. Trazhenkov, W.P. West, and N. Brooks, The Performance of Thick B4C Coatings on Graphite Divertor Tiles in the Diii-D Tokamak. *J. Nucl. Mater.*, 1996, **237**, p 787-790
76. F. Scaffidi-Argentina, G.R. Longhurst, V. Shestakov, and H. Kawamura, The Status of Beryllium Technology for Fusion. *J. Nucl. Mater.*, 2000, **283**, p 43-51
77. R.G. Castro, P.W. Stanek, K.E. Elliott, J.D. Cotton, and R.D. Watson, Optimizing the Thermal-Conductivity of Vacuum Plasma-Sprayed Beryllium for Fusion Applications. *J. Nucl. Mater.*, 1995, **226**(1-2), p 170-177
78. R.G. Castro, A.H. Bartlett, K.J. Hollis, and R.D. Fields, The Effect of Substrate Temperature on the Thermal Diffusivity and Bonding Characteristics of Plasma Sprayed Beryllium. *Fus. Eng. Des.*, 1997, **37**(2), p 243-252
79. R.G. Castro, K.E. Elliot, R.D. Watson, D.L. Youchison, and K.T. Slattery, Fabrication and High Heat Flux Testing of Plasma Sprayed Beryllium ITER First Wall Mock-Ups. *J. Nucl. Mater.*, 1998, **263**, p 252-257
80. K.J. Hollis, Plasma Sprayed Beryllium Mock Up Final Report, EFDA Report FIA-02-011, Los Alamos, 2004
81. R.P. Doerner, R.W. Conn, S.C. Luckhardt, F.C. Sze, and J. Won, Outgassing From and Deuterium Retention in Beryllium and Be/C Mixed-Material Plasma-Facing Components. *Fus. Eng. Des.*, 2000, **49**, p 183-188
82. G. Rigon and F. Brossa, Electron Beam Disruption Simulation on Coated Materials. *J. Nucl. Mater.*, 1992, **191-194**(1), p 460-464
83. R.A. Neiser, R.D. Watson, G.R. Smolik, and K.J. Hollis, An Evaluation of Plasma Sprayed Tungsten for Fusion Reactors, *Thermal Spray Coatings: Research, Design and Applications*, C.C. Berndt and T.F. Bernecki, Ed., June 7-11, 1993 (Anaheim, CA), ASM International, 1993, p 303-308
84. S. Boirelavigne, C. Moreau, and R.G. Saintjacques, The Relationship between the Microstructure and Thermal-Diffusivity of Plasma-Sprayed Tungsten Coatings. *J. Thermal Spray Technol.*, 1995, **4**(3), p 261-267
85. W. Mallener, W. Hohenauer, and D. Stoever, Tungsten Coatings for Nuclear Fusion Devices, *Thermal Spray: Practical Solutions for Engineering Problems*, C.C. Berndt, Ed., Oct 7-11, 1996 (Cincinnati, OH), ASM International, 1996, p 1-6

86. C. Garciarosales, P. Franzen, H. Plank, J. Roth, and E. Gauthier, Re-Emission and Thermal Desorption of Deuterium From Plasma Sprayed Tungsten Coatings for Application in ASDEX-Upgrade. *J. Nucl. Mater.*, 1996, **237**, p 803-808
87. B. Riccardi, A. Pizzuto, A. Orsini, S. Libera, E. Visca, L. Bertamini, F. Casadei, E. Severini, R. Montanari, R. Vesprini, P. Varone, G. Filacchioni, and N. Litunovsky, Tungsten Thick Coatings for Plasma Facing Components, *Proc. 18th Symp. on Fusion Technology*, B. Beaumont, P. Libeyre, B. de Gentile, and G. Tonon, Eds. (Marseille, France), CEA, 1998, p 223-226
88. G. Maddaluno, F. Pierdominici, and M. Vittori, Behaviour of a Tungsten Coated Molybdenum Poloidal Limiter in FTU Tokamak. *J. Nucl. Mater.*, 1997, **241**, p 908-913
89. W. Hohenauer, H. Bolt, J. Linke, and W.K.W.M. Mallener, Manufacturing and Testing of Actively Cooled Test Limiters for Textor Made of an LPPS Tungsten-Coated TZM Heat Sink. *Fusion Technol.*, 1998, **34**(1), p 18-27
90. A. Cavasin, T. Brzezinski, S. Grenier, M. Smagorinski, and P. Tsantrizos, W and B4C Coatings for Nuclear Fusion Reactors, *Thermal Spray: Meeting the Challenges of the 21st Century*, C. Coddet, Ed., May 25-29, 1998 (Nice, France), ASM International, 1998, p 957-961
91. M. Rodig, E. Ishitsuka, A. Gervash, H. Kawamura, J. Linke, N. Litunovski, and M. Merola, High Heat Flux Performance of Neutron Irradiated Plasma Facing Components. *J. Nucl. Mater.*, 2002, **307-311**(1), p 53-59
92. X. Liu, S. Tamura, K. Tokunaga, N. Yoshida, N. Noda, L. Yang, and Z. Xu, High Heat Flux Properties of Pure Tungsten and Plasma Sprayed Tungsten Coatings. *J. Nucl. Mater.*, 2004, **329-333**, p 687-691
93. H. Greuner, H. Bolt, B. Boswirth, S. Lindig, W. Kuhnlein, T. Huber, K. Sato, and S. Suzuki, Vacuum Plasma-sprayed Tungsten on EUROFER and 316L: Results of characterisation and Thermal Loading Tests. *Fus. Eng. Des*, 2005, **75-79**(0), p 333-338
94. H.-K. Kang, Thermal Properties of Plasma-Sprayed Tungsten Deposits. *J. Nucl. Mater.*, 2004, **335**(1), p 1-4
95. J. Matejicek, Y. Koza, and V. Weinzettl, Plasma Sprayed Tungsten-based Coatings and their Performance Under Fusion Relevant Conditions. *Fus. Eng. Des.*, 2005, **75-79**(0), p 395-399
96. J. Matejicek, V. Weinzettl, E. Dufkova, V. Piffl, and V. Perina, Plasma Sprayed Tungsten-based Coatings and their Usage in Edge Plasma Region of Tokamaks, *Euromat*, (Prague), Acta Technica, 2006, **51**(2), p 179-191
97. J. Matejicek, K. Neufuss, D. Kolman, O. Chumak, and V. Brozek, Development and Properties of Tungsten-Based Coatings Sprayed by WSP(R), *Thermal Spray Connects: Explore its Surfacing Potential!*, May 2-4, 2005 (Basel, Switzerland)**,** DVS, 2005, p 634-640
98. A. Warren, A. Nylund, and I. Olefjord, Oxidation of Tungsten and Tungsten Carbide in Dry and Humid Atmospheres. *Int. J. Refract. Met.Hard Mater.*, 1996, **14**(5-6), p 345-353
99. K. Neufuss, V. Brozek, and J. Matejicek, Tungsten-Based Protective Coating and a Method of its Preparation, Czech patent application PV 2005-276, April 29, 2005
100. C. Moreau, P. Fargier-Richard, R.G. Saint-Jacques, and P. Cielo, Thermal-Diffusivity of Plasma-Sprayed Tungsten Coatings. *Surf. Coat. Technol.*, 1993, **61**(1-3), p 67-71
101. H.-K. Kang, Microstructures of High Volume SiC Reinforced Tungsten Composites Produced by Plasma Spray. *Scr. Mater.*, 2004, **51**(11), p 1051-1055
102. J.H. You and H. Bolt, Analysis of Singular Interface Stresses in Dissimilar Material Joints for Plasma Facing Components. *J. Nucl. Mater.*, 2001, **299**(1), p 1-8
103. A. Salito, M. Tului, and F. Casadei, Numerical Simulation of the Internal Stresses of Thick Tungsten Coating Deposited by Vacuum Plasma Spraying on Copper Substrate, *Proc. 18th Symp. on Fusion Technology*, B. Beaumont, P. Libeyre, B. de Gentile, and G. Tonon, Ed. (Marseille, France), CEA, 1998, p 165-168
104. X. Liu, N. Yoshida, N. Noda, F. Zhang, Z.Y. Xu, and Y. Liu, Erosion and Erosion Products of Tungsten and Carbon-Based Materials Irradiated by a High Energy Electron Beam. *J. Nucl. Mater.*, 2003, **313**, p 399-403
105. Y. Koza, E. Berthe, E. Lehmann, J. Linke, M. Rodig, E. Wessel, and L. Singheiser, Formation of Dust Particles Under the Influence of Intense Thermal Loads. *J. Nucl. Mater.*, 2004, **329-333**(1), p 706-710
106. K. Tokunaga, N. Yoshida, N. Noda, Y. Kubota, S. Inagaki, R. Sakamoto, T. Sogabe, and L. Plochl, Behavior of Plasma-Sprayed Tungsten Coatings on CFC and Graphite Under High Heat Load. *J. Nucl. Mater.*, 1999, **269**, p 1224-1229
107. I. Bobin Vastra, B. Schedler, M. Merola, F. Jacquinot, A. Cottin, D. Cauvin, M. Febvre, and Y. Leblanc, Manufacturing of Prototype Components for the ITER Divertor Baffle. *Fus. Eng. Des.*, 2003, **66-68**, p 341-346
108. C. Garciarosales, S. Deschka, W. Hohenauer, R. Duwe, E. Gauthier, J. Linke, M. Lochter, W.K.W.M. Mallener, L. Plochl, P. Rodhammer, and A. Salito, High-Heat-Flux Loading of Tungsten Coatings on Graphite Deposited by Plasma Spray and Physical Vapor Deposition. *Fusion Technol.*, 1997, **32**(2), p 263-276
109. H. Maier, S. Kotterl, K. Krieger, R. Neu, and M. Balden, Performance of Tungsten Coatings as Plasma Facing Components Used in ASDEX Upgrade. *J. Nucl. Mater.*, 1998, **263**, p 921-926
110. R. Neu, R. Dux, A. Geier, O. Gruber, A. Kallenbach, K. Krieger, H. Maier, R. Pugno, V. Rohde, and S. Schweizer, Tungsten as Plasma-Facing Material in ASDEX Upgrade. *Fus. Eng. Des.*, 2003, **65**(3), p 367-374
111. K. Krieger, J. Likonen, M. Mayer, R. Pugno, V. Rohde, and E. Vainonen-Ahlgren, Tungsten Redistribution Patterns in ASDEX Upgrade. *J. Nucl. Mater.*, 2005, **337-339**, p 10-16
112. D.A. Buchenauer, B.E. Mills, R. Wood, S. Woodruff, D.N. Hill, E.B. Hooper, D.F. Cowgill, M.W. Clift, and N.Y. Yang, Characterization and Conditioning of SSPX Plasma Facing Surfaces. *J. Nucl. Mater.*, 2001, **290**, p 1165-1170
113. V. Weinzettl, J. Matejicek, V. Piffl, and S. Polosatkin, First Tests of Plasma Sprayed Tungsten Specimens in CASTOR Tokamak Discharges, *31st EPS Conference on Plasma Physics*, (London), 2004, paper p 5.139
114. R.A. Anderl, R.J. Pawelko, M.R. Hankins, G.R. Longhurst, and R.A. Neiser, Hydrogen Permeation Properties of Plasma-Sprayed Tungsten. *J. Nucl. Mater.*, 1994, **215**, p 1416-1420
115. M. Rubel, V. Philipps, A. Pospieszczyk, T. Tanabe, and S. Kotterl, Overview of Fuel Retention in Composite and Tungsten Limiters. *J. Nucl. Mater.*, 2002, **307**, p 111-115
116. R.G. Castro, K.J. Hollis, C.J. Maggiore, A. Ayala, B.D. Bartram, and R.P. Doerner, Negative Transferred Arc Cleaning: A Method for Roughening and Removing Surface Contamination From Beryllium and Other Metallic Surfaces. *Fusion Technol.*, 2000, **38**(3), p 369-375
117. H. Maier, J. Luthin, M. Balden, J. Linke, F. Koch, and H. Bol, Properties of Tungsten Coatings Deposited onto Fine Grain Graphite by Different Methods. *Surf. Coat. Technol.*, 2001, **142**, p 733-737
118. C. Fazio, K. Stein-Fechner, E. Serra, H. Glasbrenner, and G. Benamati, Investigation on the Suitability of Plasma Sprayed Fe-Cr-Al Coatings as Tritium Permeation Barrier. *J. Nucl. Mater.*, 1999, **273**(3), p 233-238
119. T. Terai, Research and Development on Ceramic Coatings for Fusion Reactor Liquid Blankets. *J. Nucl. Mater.*, 1997, **248**, p 153-158
120. A. Perujo, K.S. Forcey, and T. Sample, Reduction of Deuterium Permeation Through DIN 1.4914 Stainless Steel (MANET) by Plasma-Spray Deposited Aluminium. *J. Nucl. Mater.*, 1993, **207**, p 86-91
121. A. Perujo and K.S. Forcey, Tritium Permeation Barriers for Fusion Technology. *Fus. Eng. Des.*, 1995, **28**, p 252-257
122. G.W. Hollenberg, E.P. Simonen, G. Kalinin, and A. Terlain, Tritium Hydrogen Barrier Development. *Fus. Eng. Des.*, 1995, **28**, p 190-208
123. A. Perujo, E. Serra, H. Kolbe, and T. Sample, Hydrogen Permeation Rate Reduction by Post-Oxidation of Aluminide Coatings on DIN 1.4914 Martensitic Steel (Manet). *J. Nucl. Mater.*, 1996, **237**, p 1102-1106

124. T. Sample, A. Perujo, H. Kolbe, and B. Mancinelli, The Hydrogen Permeation Behaviour of Aluminised Coated Martensitic Steels Under Gaseous Hydrogen, Liquid Pb-17Li/Hydrogen and Cyclic Tensile Load. *J. Nucl. Mater.*, 2000, **283**, p 1272-1276
125. G. Benamati, C. Chabrol, A. Perujo, E. Rigal, and H. Glasbrenner, Development of Tritium Permeation Barriers on Al Base in Europe. *J. Nucl. Mater.*, 1999, **272**, p 391-395
126. H. Glasbrenner, J. Konys, Z. Voss, and O. Wedemeyer, Corrosion Behaviour of Al Based Tritium Permeation Barriers in Flowing Pb-17Li. *J. Nucl. Mater.*, 2002, **307-311**, p 1360-1363
127. C. Racault, E. Serra, and P. Fenici, Reduction of Deuterium Permeation Through SiC/SiC Composites by Plasma-Spray Deposited Eutectic Al-Si. *J. Nucl. Mater.*, 1995, **227**(1-2), p 50-57
128. T. Leguey, N. Baluc, F. Jansen, and M. Victoria, Characterization of Hydrogen Barrier Coatings for Titanium-Base Alloys. *J. Nucl. Mater.*, 2002, **307**, p 1329-1333
129. G. Federici, R. Causey, P.L. Andrew, and C.H. Wu, Tritium Retention in Candidate Next-Step Protection Materials - Engineering Key Issues and Research Requirements. *Fus. Eng. Des.*, 1995, **28**, p 136-148
130. D. Hildebrandt, M. Akbi, B. Juttner, and W. Schneider, Deuterium Trapping in Divertor Tiles of ASDEX-Upgrade. *J. Nucl. Mater.*, 1999, **269**, p 532-537
131. S. Malang, H.U. Borgstedt, E.H. Farnum, K. Natesan, and I.V. Vitkovski, Development of Insulating Coatings for Liquid-Metal Blankets. *Fus. Eng. Des.*, 1995, **27**, p 570-586
132. T. Terai, T. Yoneoka, H. Tanaka, A. Suzuki, S. Tanaka, M. Nakamichi, H. Kawamura, K. Miyajima, and Y. Harada, Compatibility of Yttria (Y_2O_3) With Liquid Lithium. *J. Nucl. Mater.*, 1996, **237**, p 1421-1426
133. C. Kinoshita and S.J. Zinkle, Potential and Limitations of Ceramics in Terms of Structural and Electrical Integrity in Fusion Environments. *J. Nucl. Mater.*, 1996, **237**, p 100-110
134. M. Nakamichi, H. Kawamura, T. Terai, and S. Tanaka, Characterization of Y_2O_3 Coating for Liquid Blanket. *J. Nucl. Mater.*, 1997, **248**, p 165-169
135. M. Nakamichi, H. Kawamura, K. Miyajima, Y. Harada, and R. Oyamada, Trial Fabrication and Preliminary Characterization of $MgO.Al_2O_3$ Coating. *J. Nucl. Mater.*, 1996, **237**, p 1427-1430
136. M. Nakamichi, T. Takabatake, and H. Kawamura, Material Design of Ceramic Coating by Plasma Spray Method. *Fus. Eng. Des.*, 1998, **41**, p 143-147
137. M. Nakamichi and H. Kawamura, Out-of-Pile Characterization of Al_2O_3 coating as Electrical Insulator. *Fus. Eng. Des.*, 2001, **58-59**, p 719-723
138. A. Morono and E.R. Hodgson, Radiation Induced Conductivity and Surface Electrical Degradation of Plasma Sprayed Spinel for NBI Systems. *Fus. Eng. Des.*, 2005, **75-79**(0), p 1075-1078
139. F. Elio, ITER IT Garching, Personal Communication, 2004
140. L.F. Moreschi, P. Rossi, M. Agostini, S. Storai, and A.T. Peacock, Full Scale Electrical Insulation Coating Development. *Fus. Eng. Des.*, 2003, **69**(1-4), p 303-307
141. B.C. Odegard, C.H. Cadden, R.D. Watson, and K.T. Slattery, A Review of the US Joining Technologies for Plasma Facing Components in the ITER Fusion Reactor. *J. Nucl. Mater.*, 1998, **263**, p 329-334
142. C.H. Cadden and B.C. Odegard, Aluminum-Assisted Joining of Beryllium to Copper for Fusion Applications. *Fus. Eng. Des.*, 1997, **37**(2), p 287-298
143. R.E. Nygren, D.L. Youchison, J.M. McDonald, T.J. Lutz, J.S. O'Dell, K. Ezato, and K. Sato, High heat flux tests of mockups with W rod armor. *Fus. Eng. Des.*, 2003, **66-68**, p 353-357
144. Y. Itoh, M. Takahashi, and H. Takano, Design of Tungsten/Copper Graded Composite for High Heat Flux Components Fus. *Eng. Des.*, 1996, **31**(4), p 279-289
145. S. Ueda, Elastoplastic Analysis of W-Cu Functionally Graded Materials Subjected to a Thermal Shock by Micromechanical Model. *J. Thermal Stresses.*, 2001, **24**, p 631-649
146. J. Chapa and I. Reimanis, Modeling of Thermal Stresses in a Graded Cu/W Joint. *J. Nucl. Mater.*, 2002, **303**(2-3), p 131-136
147. G. Pintsuk, S.E. Brunings, J.-E. Doring, J. Linke, I. Smid, and L. Xue, Development of W/Cu—Functionally Graded Materials. *Fus. Eng. Des.*, 2003, **66-68**, p 237-240
148. J.-E. Doring, R. Vassen, G. Pintsuk, and D. Stover, The Processing of Vacuum Plasma-Sprayed Tungsten-Copper Composite Coatings For High Heat Flux Components. *Fus. Eng. Des.*, 2003, **66-68**, p 259-263
149. G. Pintsuk, J.-E. Döring, W. Hohenauer, J. Linke, J. Matejicek, I. Smid, and F. Tietz, Microstructural and Mechanical Properties Of Plasma Sprayed W/Cu-Graded Composites for Extreme Thermal Conditions, *World Congress on Powder Metallurgy & Particulate Materials (PM2TEC)*, (Las Vegas), Metal Powder Industries Federation, 2003, p 6.107-6.118
150. G. Pintsuk, I. Smid, J.-E. Doring, W. Hohenauer, and J. Linke, Fabrication and Characterization of Vacuum Plasma Sprayed W/Cu-Composites for Extreme Thermal Conditions, *J. Mater. Sci.*, 2005, in press
151. K.T. Slattery and D.E. Driemeyer, Process of Bonding Copper and Tungsten, US patent US5988488, November 23, 1999
152. R. Montanari, B. Riccardi, R. Volterri, and L. Bertamini, Characterisation of Plasma Sprayed W Coatings on a CuCrZr Alloy for Nuclear Fusion Reactor Applications. *Mater. Lett.*, 2002, **52**(1-2), p 100-105
153. R.D. Seals, C.J. Swindeman, and R.L. White, Thermal Spray Deposition and Evaluation of Low-Z Coatings., *Thermal Spray: Practical Solutions for Engineering Problems*, C.C. Berndt, Ed., Oct 7-11, 1996 (Cincinnati, OH), ASM International, 1996, p 13-19
154. L.H. Taylor and L. Green, Tantalum Coatings for Inertial Confinement Fusion Dry Wall Designs, Fus. *Eng. Des.*, 1996, **32-33**, p 105-111
155. S. Nanobashvili, J. Matějíček, F. Žáček, J. Stöckel, P. Chráska, and V. Brožek, Plasma Sprayed Coatings for RF Wave Absorption. *J. Nucl. Mater.*, 2002, **307-311**, p 1334-1338
156. J. Matějíček and P. Chráska, Plasma Spraying of B4C for Fusion Applications, Report on EFDA task no. DV4/04 (TW0), Prague, 2000
157. J. Linke, F. Escourbiac, I.V. Mazul, R. Nygren, M. Rödig, J. Schlosser, and S. Suzuki, High Heat Flux Testing of Plasma Facing Materials and Components - Status and Perspectives for ITER Related Activities, *12th International Conference on Fusion Reactor Materials* (Santa Barbara, CA), 2005, to be published in J. Nucl. Mater
158. M. Rodig, M. Akiba, P. Chappuis, R. Duwe, M. Febvre, A. Gervash, J. Linke, N. Litounovsky, S. Suzuki, B. Wiechers, and D.L. Youchison, Comparison of Electron Beam Test Facilities for Testing of High Heat Flux Components. *Fus. Eng. Des.*, 2000, **51-52**, p 715-722
159. M. Rödig, I. Bobin-Vastra, S. Cox, F. Escourbiac, A. Gervash, A. Kapoustina, W. Kuehnlein, V. Kuznetsov, M. Merola, R. Nygren, and D.L. Youchison, Testing of Actively Cooled Mock-Ups in Several High Heat Flux Facilities an International Round Robin Test. *Fus. Eng. Des.*, 2005, **75-79**, p 303-306
160. H. Greuner, H. Bolt, B. Böswirth, T. Franke, P. McNeely, S. Obermayer, N. Rust, and R. Süß, Design, Performance and Construction of a 2 MW Ion Beam Test Facility for Plasma Facing Components. *Fus. Eng. Des.*, 2005, **75-79**, p 345-350
161. G. Hoffmann and E. Eggert, First Wall Test Facility FIWATKA, Kernforschungszentrum Karlsruhe report KfK 5381, Karlsruhe, 1994
162. J.G. Van derLaan, Effects of pulsed-laser radiation on first-wall materials. *J. Nucl. Mater.*, 1989, **162-164**, p 964-969
163. Y. -H. Ling, J.-T. Li, C.-C. Ge, and X.-D. Bai, Fabrication and Evaluation of SiC/Cu Functionally Graded Material Used for Plasma Facing Components in a Fusion Reactor. *J. Nucl. Mater*, 2002, **303**(2-3), p 188-195
164. G. Federici, A. Zhitlukhin, N. Arkhipov, R. Giniyatulin, N. Klimov, I. Landman, V. Podkovyrov, V. Safronov, A. Loarte, and M. Merola, Effects of ELMs and Disruptions on ITER Divertor Armour Materials. *J. Nucl. Mater.*, 2005, **337-339**(1-3), p 684-690
165. T.J. Renk, Materials Modifications Using Intense Ion Beams. *Proc. IEEE*, 2004, **92**, p 1057-1081

166. H. Wurz, B. Bazylev, I. Landman, S. Pestchanyi, and V. Safronov, Macroscopic Erosion of Divertor and First Wall Armour in Future Tokamaks. *J. Nucl. Mater.*, 2002, **307**, p 60-68
167. F. Escourbiac A. Durocher V. Casalegno, and S. Constans, Application of Lock-in Technique to CFC Armoured Plasma Facing Components Inspection, *12th International Conference on Fusion Reactor Materials*, (Santa Barbara CA), 2005, to be published in *J. Nucl. Mater*
168. H. Traxler, J. Schlosser, A. Durocher, B. Schedler, T. Huber, and A. Zabernig, A New Inspection Method for Plasma Facing Components. *Phys. Scr*, 2004, **T111**, p 203-205
169. J. Schlosser, CEA Cadarache, Personal communication, 2005
170. A.C. Aiello and G. Benamati, An Overview on Tritium Permeation Barrier Development for WCLL Blanket Concept, *J. Nucl. Mater.* **329-333**, 2004, p 1398-1402, and personal communication